

On the Inference of Spatial Continuity using Spartan Random Field Models

Samuel Elogne* and Dionissios T. Hristopoulos†

Department of Mineral Resources Engineering

Technical University of Crete

Chania 73100, Greece

Abstract

This paper addresses the inference of spatial dependence in the context of a recently proposed framework. More specifically, the paper focuses on the estimation of model parameters for a class of generalized Gibbs random fields [12], i.e., Spartan Spatial Random Fields (SSRFs). The problem of parameter inference is based on the minimization of a distance metric. The latter involves a specifically designed distance between sample constraints (variance, generalized “gradient” and “curvature”) and their ensemble counterparts. The general principles used in the construction of the metric are discussed and intuitively motivated. In order to enable calculation of the metric from sample data, estimators for generalized “gradient” and “curvature” constraints are constructed. These estimators, which are not restricted to SSRFs, are formulated using compactly supported kernel functions. An intuitive method for kernel bandwidth selection is proposed. It is proved that the estimators are asymptotically unbiased and consistent for differentiable random fields, under specified regularity conditions. For continuous but non-differentiable random fields, it is shown that the estimators are asymptotically consistent. The bias is calculated explicitly for different kernel functions. The performance of the sample constraint estimators and the SSRF inference process are investigated by means of numerical simulations.

PACS numbers:

Keywords: non-parametric, inverse problem, optimization, simulation

*Electronic address: elogne@mred.tuc.gr

†Electronic address: dionisi@mred.tuc.gr; URL: <http://www.mred.tuc.gr/home/hristopoulos/dionisi.html>

I. INTRODUCTION

Spatial Random Fields (SRF's) have a wide range of applications in subsurface hydrology [6, 18, 22], petroleum engineering [10], environmental data analysis [3, 17, 23], mining exploration and reserves estimation [1, 7], and environmental health [4] among other fields. From the applications viewpoint, the main goals are first to characterize the spatial continuity of such processes, and then to exploit the continuity for spatial estimation (prediction) and simulation. A methodological problem of continuing interest is the inference of the random field parameters that characterize the spatial continuity from the experimental data. The latter are typically distributed on irregular sampling grids.

This paper seeks to address the issue of random field inference within the context of a specific model, the Fluctuation-Gradient-Curvature (FGC) Spartan Spatial Random Field (SSRF), which was introduced in [12]. SSRFs result from a convolution of a kernel function with an underlying SRF that may include non-resolved fine-scale detail at length scales below λ . The kernel function acts as a low-pass filter that suppresses the spectral component of fluctuations above a cutoff wavevector k_c . The removed part corresponds to sub-resolution scales. We will denote *sample averages* with a horizontal bar over the averaged quantity, and *ensemble averages* with the mathematical expectation symbol, i.e., $m_X = \mathbb{E}[X_\lambda(\mathbf{s})]$. Without loss of generality in the following it is assumed that $m_X = 0$.

Let the data be given by the measurements $\mathbf{X}^* \equiv \{X_1^*, \dots, X_n^*\}$, of the scalar quantity X at the set of sampling locations $\mathbf{S}_m \equiv \{\mathbf{s}_1, \dots, \mathbf{s}_n\}$ in the domain $\Omega_n \in \mathbb{R}^d$. The area enclosed by the convex hull of Ω_n is denoted by $|\Omega_n|$. We assume that the data can be modeled as a *sample* (realization) of $X_\lambda(\mathbf{s})$, which is a Gaussian, weakly stationary, isotropic FGC-SSRF. The isotropic assumption is not a major restriction, since under certain conditions the anisotropic parameters can be established and isotropic conditions can be restored by rotation and rescaling transformations [11, 13, 14]. The isotropic FGC-SSRF involves the *parameter set* $\boldsymbol{\theta} = (\eta_0, \eta_1, \xi, k_c)$: the *scale coefficient* η_0 determines the variance, the *shape coefficient* η_1 determines the shape of the covariance function, the *characteristic length* ξ determines the range of spatial dependence, and k_c is a *wavevector cutoff* related to the resolution scale λ [12].

Regarding parameter inference, the main idea introduced in [12] and further elaborated here, is that the SSRF model parameters can be estimated by matching sample constraints

and their ensemble counterparts. The model parameters are determined by treating the sample constraints as estimators of the respective stochastic constraints. This perspective relies on the validity of the *ergodic hypothesis* [19, 25].

The constraint matching idea is similar to the standard approach, in which the experimental variogram is matched with various model functions to determine an optimal model of spatial continuity. However, there are significant differences between the two approaches. (1) In the SSRF approach the number of estimated constraints is small (four in the case of the FGC-SSRF). This is due to the efficient parametrization of spatial dependence in the FGC-SSRF, which is based on interactions instead of the covariance matrix. In contrast, variogram modeling attempts to match the entire functional dependence of the variogram function. (2) The FGC-SSRF includes a family of covariance functions that account for various types of spatial continuity [12, 16]. Hence, in practice fitting the sample constraints with one SSRF model may be sufficient. In contrast, the experimental variogram is fitted with a number of model functions to determine the “optimal” spatial model. (3) The SSRF sample constraints focus on the short-range behavior of spatial continuity. This is motivated by two observations: in geostatistical applications, the long-range behavior can only be estimated with significant uncertainty; in addition, it is known that the long-range behavior does not have a significant impact on optimal linear prediction in regions where the field is densely sampled [24]. (4) The computational complexity of SSRF constraint calculations, at least on regular grids, is $O(mn)$, where m is $o(n)$ and depends on the kernel bandwidth, while for variogram calculations the respective complexity is at best $O(n \log n)$ if tree-based structures are used, or $O(n^2)$ using standard methods [12].

The main results obtained in this paper include the following: (1) Generalized gradient and curvature estimators are formulated in terms of kernel averages, and a consistent method for selecting the kernel bandwidths is proposed. The generalized gradient and curvature estimators have a wider scope than the FGC-SSRF model: They are defined for both differentiable and continuous (but non-differentiable) spatial models. In the differentiable case, the estimators are defined in terms of finite-difference approximations of the respective derivatives. In the continuous case, the finite differences are not divided by the corresponding length spacing (step) in order to obtain asymptotically well defined quantities. (2) Convergence properties for the generalized gradient and curvature estimators are proved. (3) The constraint-based parameter inference procedure introduced in [12] is improved by adding

a constraint that eliminates the nonlinear dependence of the model variance on the FGC-SSRF parameters. (4) Numerical simulations establish the performance of the constraints estimators and the parameter inference procedure.

The remaining of this paper is structured as follows: An introduction to the FGC-SSRF in continuum space is given in Section (II). In Section (III) the definition of the sample constraints on regular grids is reviewed. This is followed by the definition of generalized stochastic constraints for the FGC-SSRF in Section (IV). Generalized sample constraints for the gradient and curvature are defined in Section (V). Theorems establishing the convergence of the constraint estimators are stated and proved in Section (VI). Subsequently, the parameter inference process developed in [12] is reviewed and refined in Section (VII). Finally, numerical simulations are used to validate the estimators and the parameter inference process in Section (VIII).

II. REVIEW OF THE FGC-SSRF MODEL

In general, a *Gibbs* random field has the following joint probability density function (p.d.f.)

$$f_x[X_\lambda(\mathbf{s}); \boldsymbol{\theta}] = \frac{\exp \{-H[X_\lambda(\mathbf{s}); \boldsymbol{\theta}]\}}{Z(\boldsymbol{\theta})}, \quad (1)$$

where $H[X_\lambda(\mathbf{s}); \boldsymbol{\theta}]$ is the *energy functional*, $\boldsymbol{\theta}$ is a set of *model parameters*, and the constant $Z(\boldsymbol{\theta})$, called the *partition function* is the p.d.f. normalization factor obtained by integrating $\exp \{-H[X_\lambda(\mathbf{s}); \boldsymbol{\theta}]\}$ over all the realizations of the SRF. The FGC p.d.f. in R^d is determined from the equation:

$$H_{\text{fgc}}[X_\lambda(\mathbf{s}); \boldsymbol{\theta}] = \frac{1}{2\eta_0\xi^d} \int d\mathbf{s} h_{\text{fgc}} [X_\lambda(\mathbf{s}); \boldsymbol{\theta}'], \quad (2)$$

where $\boldsymbol{\theta}' = (\eta_1, \xi, k_c)$, and h_{fgc} is the normalized (to $\eta_0 = 1$) local energy density at point \mathbf{s} . The functional $h_{\text{fgc}} [X_\lambda(\mathbf{s}); \boldsymbol{\theta}']$ is given *in the continuum* by the following expression

$$h_{\text{fgc}} [X_\lambda(\mathbf{s}); \boldsymbol{\theta}'] = [X_\lambda(\mathbf{s})]^2 + \eta_1 \xi^2 [\nabla X_\lambda(\mathbf{s})]^2 + \xi^4 [\nabla^2 X_\lambda(\mathbf{s})]^2, \quad (3)$$

The functional (3) is permissible if the resulting covariance function is positive definite, i.e., if it satisfies *Bochner's theorem* [2]. Permissibility constrains the value of η_1 (see [12],[16]).

The explicit, albeit non-linear, dependence of the p.d.f. on three physically meaningful parameters, η_0, η_1, ξ , instead of three linear coefficients multiplying the terms $[X_\lambda(\mathbf{s})]^2$, $[\nabla X_\lambda(\mathbf{s})]^2$ and $[\nabla^2 X_\lambda(\mathbf{s})]^2$, simplifies the parameter inference problem and allows intuitive initial guesses for the parameters.

The FGC model has a particularly simple expression in Fourier space. If the Fourier transform of the covariance function is defined by means of

$$\tilde{G}_{\mathbf{x};\lambda}(\mathbf{k}; \boldsymbol{\theta}) = \int d\mathbf{r} e^{-i\mathbf{k}\cdot\mathbf{r}} G_{\mathbf{x};\lambda}(\mathbf{r}; \boldsymbol{\theta}), \quad (4)$$

then the energy functional in Fourier space is given by

$$H_{\text{fgc}}[X_\lambda(\mathbf{s}); \boldsymbol{\theta}] = \frac{1}{2(2\pi)^d} \int d\mathbf{k} \tilde{X}_\lambda(\mathbf{k}) \tilde{G}_{\mathbf{x};\lambda}^{-1}(\mathbf{k}; \boldsymbol{\theta}) \tilde{X}_\lambda(-\mathbf{k}). \quad (5)$$

The interaction is diagonal in Fourier space, i.e., the *precision matrix* $\tilde{G}_{\mathbf{x};\lambda}^{-1}(\mathbf{k}; \boldsymbol{\theta})$ couples only components with equal wavevectors. For a real-valued SSRF $X_\lambda(\mathbf{s})$ it follows that $\tilde{X}_\lambda(-\mathbf{k}) = \tilde{X}_\lambda^\dagger(\mathbf{k})$. Since Bochner's theorem guarantees the non-negativity of the covariance spectral density, it follows from (5) that the energy is a non-negative functional.

The covariance spectral density follows from the expression:

$$\tilde{G}_{\mathbf{x};\lambda}(\mathbf{k}; \boldsymbol{\theta}) = \frac{|\tilde{Q}_\lambda(\mathbf{k})|^2 \eta_0 \xi^d}{1 + \eta_1 (k\xi)^2 + (k\xi)^4} \quad (6)$$

where $\tilde{Q}_\lambda(\mathbf{k})$ is the Fourier transform of the coarse-graining kernel, which determines how the fluctuations are cut off at the resolution scale λ [12]. For isotropic SSRF's, $\tilde{Q}_\lambda(\mathbf{k})$ has no directional dependence. In [12, 15], a kernel having a boxcar spectral density with a sharp wavevector cutoff at k_c was used. This kernel leads to a band-limited covariance spectral density $\tilde{G}_{\mathbf{x};\lambda}(\mathbf{k}; \boldsymbol{\theta})$.

III. GENERALIZED ENERGY FUNCTIONAL

The energy density defined by Eq. (3) is valid in the continuum, and for differentiable SRFs. Generalized versions of the functional that are valid on regular lattices can be defined. For example:

Definition 1 We define the local energy terms S_0 , $S_1(a_1)$, and $S_2(a_2)$, $\forall \mathbf{s} \in \mathbb{L}_d$, as follows:

$$S_0 = [X_\lambda(\mathbf{s})]^2, \quad S_1(a_1) = \sum_{i=1}^d \left[X_\lambda(\mathbf{s} + a_1 \tilde{\mathbf{e}}_i) - X_\lambda(\mathbf{s}) \right]^2 / a_1^2$$

$$S_2(a_2) = \sum_{i,j=1}^d \Delta_2^{(i)} [X_\lambda(\mathbf{s})] \Delta_2^{(j)} [X_\lambda(\mathbf{s})],$$

where $\Delta_2^{(i)}$ is the centered second-order difference operator in the direction $\tilde{\mathbf{e}}_i$, i.e.,

$$\Delta_2^{(i)} [X_\lambda(\mathbf{s})] = \left[X_\lambda(\mathbf{s} + a_2 \tilde{\mathbf{e}}_i) + X_\lambda(\mathbf{s} - a_2 \tilde{\mathbf{e}}_i) - 2X_\lambda(\mathbf{s}) \right] / a_2^2.$$

S_0 represents the square of the fluctuations, S_1 the square of the generalized gradient, and S_2 the square of the generalized curvature.

The *generalized gradient* and *curvature* terms above are expressed in terms of finite differences instead of derivatives. These terms replace the gradient and curvature in (3). On a hypercubic lattice $\mathbb{L}_d \subset \mathbb{Z}^d$ in d dimensions with step a , one obtains $a_1 = a_2 = a$. The sample counterparts of $S_i(\mathbf{s})$, $i = 0, 1, 2$, obtained by replacing $X_\lambda(\mathbf{s})$ with $X^*(\mathbf{s})$, are thus well-defined even for non-differentiable SRFs. Parameter inference is based on matching the sample constraints, $\overline{S_i(\mathbf{s})}$, with the stochastic constraints, $\mathbb{E}[S_i(\mathbf{s})]$, as shown in [12].

Definition 2 The ensemble moments $\mathbb{E}[S_0]$, $\mathbb{E}[S_1(a_1)]$ and $\mathbb{E}[S_2(a_2)]$ provide the SSRF model constraints. These can be expressed in terms of the variance $G_\lambda(0)$ and the semi-variogram function F_λ as follows:

$$\mathbb{E}[S_0] = G_\lambda(0), \tag{7}$$

$$\mathbb{E}[S_1(a_1)] := \frac{\phi_1(a_1)}{a_1^2} = \frac{c_d^{(1)}}{a_1^2} F_\lambda(a_1) \tag{8}$$

$$\mathbb{E}[S_2(a_2)] := \frac{\phi_2(a_2)}{a_2^4} = \frac{1}{a_2^4} \left[c_d^{(2)} F_\lambda(a_2) - c_d^{(3)} F_\lambda(\sqrt{2}a_2) - c_d^{(1)} F_\lambda(2a_2) \right], \tag{9}$$

where $c_d^{(1)} = 2d$, $c_d^{(2)} = 8d^2$, and $c_d^{(3)} = 4d(d-1)$.

Remark 1 The SSRF constraints are expressed in terms of the semivariogram F_λ , but this does not imply that the experimental variogram is required for determining the spatial model.

The dependence of the stochastic constraints on the SSRF parameters θ is not shown explicitly to keep the notation concise. The stochastic constraints are well defined for the FGC-SSRF, which are differentiable if k_c is finite [16]. In the case of continuous but non-differentiable models, the ratios $\phi_1(a_1)/a_1^2$ and $\phi_2(a_2)/a_2^4$ are not well defined when $a_1, a_2 \rightarrow 0$. Then, the constraints are defined in terms of the quantities $\phi_1(a_1)$ and $\phi_2(a_2)$ respectively.

IV. CONSTRAINT DEFINITIONS ON IRREGULAR GRIDS

In most geostatistical applications the available sample is distributed on an irregular sampling grid. In order to infer the model parameters, suitable stochastic and sample-based constraints need to be defined. On regular grids the lattice symmetry leads to obvious choices for the *distance increments* (steps) a_1 and a_2 and the finite differences. On irregular grids, we formulate the sample gradient and curvature constraints using kernel averages. We also define steps a_1 and a_2 , suitable for general sampling point distributions. In addition, the kernel bandwidths are selected so as to yield good asymptotic properties for the generalized gradient and curvature estimators.

A. Stochastic FGC-SSRF Constraints

The stochastic constraints are related to the SRF model and thus do not depend on the sampling point distribution. Hence, the constraints defined in (7)-(9) can be used for irregular grids as well. The dependence of the constraints on the SSRF parameters is made explicit using the *spectral representation of the covariance function* [25]. If we define $v = (k_c \xi)^2$, $\Pi(v) = 1 + \eta_1 v + v^2$, and $w = v^{1/2} \xi^{-1}$ then for any $a > 0$ the following relations hold:

$$G_\lambda(a) = \frac{\eta_0 \xi^{d/2-1}}{2 (2\pi)^{d/2} a^{d/2-1}} \int_0^\infty dv v^{(d-2)/4} J_{d/2-1}(aw) \frac{|\tilde{Q}_\lambda(w)|^2}{\Pi(v)}. \quad (10)$$

The *variance stochastic constraint*, obtained for $a = 0$, is given by

$$\mathbb{E}[S_0] = \frac{\eta_0}{2^d \pi^{d/2} \Gamma(d/2)} \int_0^\infty dv v^{d/2-1} \frac{|\tilde{Q}_\lambda(w)|^2}{\Pi(v)}. \quad (11)$$

In general, the dependence of $\mathbb{E}[S_0]$ on η_1 and $k_c \xi$ is nonlinear [16], i.e., $\sigma_x^2 = \eta_0 g_d(\eta_1, k_c \xi)$. The function $g_d(\eta_1, k_c \xi)$ tends to an asymptotic finite bound as $k_c \xi \rightarrow \infty$. The bound is

attained with very good accuracy if $k_c \xi = q_d$, where q_d is an $O(1)$ constant that depends on d . To eliminate the dependence of the SSRF variance on η_1 and $k_c \xi$, we impose the relation

$$\eta_0 = 2^d \pi^{d/2} \Gamma(d/2) \sigma_x^2, \quad (12)$$

which is equivalent to the following normalization constraint:

$$\mathbb{E}[S'_0] = \int_0^\infty dv v^{d/2-1} \frac{|\tilde{Q}_\lambda(w)|^2}{\Pi(v)} = 1. \quad (13)$$

The stochastic constraint for the *generalized gradient* is given by

$$\mathbb{E}[S_1(a_1)] = \frac{c_d^{(1)} \sigma_x^2}{a_1^2} \int_0^\infty dv \left[v^{d/2-1} - \gamma_d v^{(d-2)/4} \frac{J_{d/2-1}(a_1 w)}{a_1^{d/2-1}} \right] \frac{|\tilde{Q}_\lambda(w)|^2}{\Pi(v)}, \quad (14)$$

where $\gamma_d = (2\xi)^{d/2-1} \Gamma(d/2)$.

Based on (9) and (10), the stochastic constraint for the *generalized curvature* is given by

$$\mathbb{E}[S_2(a_2)] = \frac{\sigma_x^2}{a_2^4} \int_0^\infty dv \frac{|\tilde{Q}_\lambda(w)|^2}{\Pi(v)} \left\{ \left[c_d^{(3)} + 3c_d^{(1)} \right] v^{d/2-1} - \gamma_d \frac{v^{(d-2)/4}}{a_2^{d/2-1}} \right. \\ \left. \left[c_d^{(2)} J_{d/2-1}(a_2 w) - c_d^{(3)} \frac{J_{d/2-1}(a_2 \sqrt{2} w)}{2^{d/4-1/2}} - c_d^{(1)} \frac{J_{d/2-1}(2a_2 w)}{2^{d/2-1}} \right] \right\}. \quad (15)$$

The selection of η_0 based on Eq. (12) increases the number of SSRF constraints to four; the other three are given by the equations (11), (14) and (15). Thus, the number of parameters matches the number of constraints.

The steps a_1 and a_2 depend on the sampling point distribution. Their selection is discussed in Section (VI) below. In general, a_2 is different from a_1 . To incorporate the spatial modelling of data from non-differentiable distributions, one should focus on the quantities $\phi_1(a_1) = a_1^2 \mathbb{E}[S_1(a_1)]$ and $\phi_2(a_2) = a_2^4 \mathbb{E}[S_2(a_2)]$ instead of $\mathbb{E}[S_1(a_1)]$ and $\mathbb{E}[S_2(a_2)]$.

V. SAMPLE CONSTRAINTS

We formulate sample constraints that provide ‘well-behaved’ estimators of the model constraints defined above. We emphasize that the following sample estimators of the generalized gradient and curvature constraints are not restricted to the FGC-SSRF model.

The variance constraint is local, i.e., it does not involve differences between neighboring points. Hence, if the distribution of the sampling points is uniform, it is sufficient to use the

classical variance estimator. To estimate a non-zero mean one can use the sample average, $\hat{m}_x = n^{-1} \sum_i^n X^*(\mathbf{s}_i)$, in view of which the sample variance $\overline{\mathcal{S}}_0$ is given by:

$$\overline{\mathcal{S}}_0 = \frac{1}{n} \sum_{i=1}^n [X^*(\mathbf{s}_i) - \hat{m}_x]^2. \quad (16)$$

Declustered estimates of the mean and the variance can be used if the sampling point distribution is non-uniform, in order to obtain unbiased estimates of the variance. However, non-ergodic fluctuations, which often dominate the estimation of the variance from a single sample, are not significantly reduced by cell declustering. Another possibility is using the kernel-based variance estimator [8], which has improved convergence properties. However, we are not aware of a systematic method for selecting the kernel bandwidth for the variance.

A. Kernel Averages of Sample Functions

To define sample-based generalized gradient and curvature constraints we use *isotropic kernel functions* $K(\mathbf{r})$ with suitably selected bandwidth parameters, h_1 (for the gradient estimator) and h_2 (for the curvature estimator). The selection of the bandwidths is guided by consistency principles that link them to the respective steps, a_1 and a_2 .

The kernel K is a bounded, positive, and compactly supported $[0, R]$ function. Hence, the moments

$$m_{K,j} = \int_0^R ds s^{j-1} K(s), \quad (17)$$

and

$$m_{K,j}^{(2)} = \int_0^R ds s^{j-1} K^2(s). \quad (18)$$

are finite for all $j \in \mathbb{Z}^+$. In addition, we define the *kernel moment ratio*:

$$B_p := \frac{m_{K,d+p}}{m_{K,d}}. \quad (19)$$

In practice non-compactly supported kernels (e.g., the Gaussian kernel,) that decrease to 0 faster than polynomially work just as well as compactly supported kernels.

The following notation is introduced to facilitate calculations with kernel averages. For $\mathbf{s}_i, \mathbf{s}_j \in \mathbf{S}_m$, $\mathbf{s}_{i,j} := \mathbf{s}_i - \mathbf{s}_j$ will denote the distance vector, and $s_{i,j} := \|\mathbf{s}_{i,j}\|$ its Euclidean norm.

The abbreviations $W_{i,j} := K(\mathbf{s}_{i,j}/h_1)$, and $Q_{i,j(r)} := K(\mathbf{s}_{i,j}/rh_2)$ where $r = 1, 2, \sqrt{2}$ will be used for the kernel weights. The weights $W_{i,j}$ and $Q_{i,j(r)}$ are random variables, due to the variability in the sampling positions.

The symbol $\sum'_{i,j}$ will denote a summation over both position indices i and j excluding the diagonal terms $i = j$. Similarly, the triple summation $\sum'_{i,j,k}$ and the quadruple summation $\sum'_{i,j,k,l}$ will exclude all the terms in which at least two indices take the same value.

Given kernel bandwidths h_1 and h_2 , and a two-point sample function $A_{i,j} = A(X_i^*, X_j^*)$ or a function of sampling positions $A_{i,j} = A(\mathbf{s}_i, \mathbf{s}_j)$, where $i, j = 1 \dots, n$, the *off-diagonal kernel-weighted averages* will be denoted by:

$$\mathbb{K}_{h_1} \{A_{i,j}\} := \sum'_{i,j} W_{i,j} A_{i,j}, \quad (20)$$

$$\mathbb{K}_{rh_2} \{A_{i,j}\} := \sum'_{i,j} Q_{i,j(r)} A_{i,j}. \quad (21)$$

The *normalized kernel average* of $A_{i,j}$ is defined by means of the equation:

$$\langle A_{i,j} \rangle_{h_1} := \frac{\mathbb{K}_{h_1} \{A_{i,j}\}}{\mathbb{K}_{h_1} \{1\}}. \quad (22)$$

More specifically, we will denote the *sample increment SRF* by means of

$$X_{i,j}^* := X^*(\mathbf{s}_i) - X^*(\mathbf{s}_j).$$

The sample function that represents the kernel average of $X_{i,j}^*$ with a kernel bandwidth h will be denoted by

$$\overline{f_X}(h) := \langle [X_{i,j}^*]^2 \rangle_h. \quad (23)$$

The random variable $\overline{f_X}(h)$ incorporates variability due to both X^* and the sampling positions.

B. Definition of Sample Gradient and Curvature Estimators

The notation introduced above is now used to define sample estimators for the squares of the generalized gradient and curvature.

Definition 3 *The sample average of the square generalized gradient is defined as follows:*

$$\overline{\mathcal{S}}_1(a_1) := \frac{c_d^{(1)}}{2a_1^2} \left\langle [X_{i,j}^*]^2 \right\rangle_{h_1} = \frac{c_d^{(1)}}{2a_1^2} \overline{f}_X(h_1) := \frac{\overline{\varphi}_1(h_1)}{a_1^2}, \quad (24)$$

where $\overline{\varphi}_1(h_1) = d \overline{f}_X(h_1)$.

The bandwidth h_1 is related to a_1 by means of the following consistency principle:

$$a_1^2 = \left\langle s_{i,j}^2 \right\rangle_{h_1}. \quad (25)$$

The step-bandwidth dependence introduced by the consistency principle is physically motivated, because only a_1 represents an actual length scale. By adopting (25), the kernel average in (24) is forced to focus on points separated by distances controlled by the step value. This makes sense for calculations of generalized gradient and curvature terms. The sample constraint defined in (24) is analogous to the respective stochastic constraint in (8). In addition, the consistency principle ensures that, for differentiable SRFs, $\overline{\mathcal{S}}_1(a_1)$ is an unbiased estimator of $\mathbb{E}[S_1(a_1)]$ (see below).

We introduced the three related quantities, $\overline{f}_X(h_1)$, $\overline{\varphi}_1(h_1)$ and $\overline{\mathcal{S}}_1(a_1)$ for the following reasons: If the observed SRF can be considered differentiable, the generalized gradient constraint $\overline{\mathcal{S}}_1(a_1)$ is well defined at the limit $a_1 \rightarrow 0$. If the observed SRF is continuous but non-differentiable the limit of $\overline{\mathcal{S}}_1(a_1)$ as $a_1 \rightarrow 0$ does not exist. In this case, it makes more sense to work with the kernel-averaged square increment, $\overline{\varphi}_1(h_1)$. To simplify the accounting it is often advantageous to work with the square increment per direction, $\overline{f}_X(h_1)$; in the isotropic case $\overline{\varphi}_1(h_1)$ and $\overline{f}_X(h_1)$ are simply proportionally related. Similar comments apply to the case of the generalized curvature constraint.

Definition 4 *The sample average of the square generalized curvature is defined as follows:*

$$\overline{\mathcal{S}}_2(a_2) := \frac{\overline{\varphi}_2(h_2)}{a_2^4} = \frac{1}{2a_2^4} \left[c_d^{(2)} \mu_1(h_2) \overline{f}_X(h_2) - c_d^{(3)} \mu_2(h_2) \overline{f}_X(\sqrt{2}h_2) - c_d^{(1)} \overline{f}_X(2h_2) \right], \quad (26)$$

the constants $\mu_1(h_2), \mu_2(h_2)$ are given by the following averages:

$$\mu_1(h_2) = \frac{c_d^{(3)} \mu_2(h_2) \left\langle s_{i,j}^2 \right\rangle_{\sqrt{2}h_2} + c_d^{(1)} \left\langle s_{i,j}^2 \right\rangle_{2h_2}}{c_d^{(2)} \left\langle s_{i,j}^2 \right\rangle_{h_2}}, \quad (27)$$

$$\mu_2(h_2) = \frac{[c_d^{(2)} + 8c_d^{(1)}] \langle s_{i,j}^4 \rangle_{h_2} + c_d^{(1)} \langle s_{i,j}^4 \rangle_{h_2} \frac{\langle s_{i,j}^2 \rangle_{2h_2}}{\langle s_{i,j}^2 \rangle_{h_2}} - c_d^{(1)} \langle s_{i,j}^4 \rangle_{2h_2}}{c_d^{(3)} \langle s_{i,j}^4 \rangle_{\sqrt{2}h_2} - c_d^{(3)} \langle s_{i,j}^4 \rangle_{h_2} \frac{\langle s_{i,j}^2 \rangle_{\sqrt{2}h_2}}{\langle s_{i,j}^2 \rangle_{h_2}}}. \quad (28)$$

The bandwidth h_2 is linked to the step by means of the consistency principle:

$$a_2^4 = \langle s_{i,j}^4 \rangle_{h_2}, \quad (29)$$

The sample constraint $\overline{\mathcal{S}}_2(a_2)$ given by (26) includes three terms that correspond to the terms in the respective stochastic constraint (9). The coefficients $\mu_1(h_2)$ and $\mu_2(h_2)$ in (26) incorporate the impact of the sampling network topology and the kernel function used. As shown in Lemma (7), Section (VID), the coefficients $\mu_1(h_2)$ and $\mu_2(h_2)$ are approximately equal to 1. Their precise form is selected to ensure that, in the case of differentiable SRFs, the generalized curvature constraint is asymptotically unbiased.

VI. ASYMPTOTIC PROPERTIES OF CONSTRAINT ESTIMATORS

The asymptotic limit corresponds to $n \rightarrow \infty$. At the limit it is assumed that $1/|\Omega_n| \rightarrow 0$. In order to establish the asymptotic properties of the sample estimators for the generalized gradient and curvature, we first present some formalism and the conditions required for the validity of the proofs.

A. Formalism

The following notation will be used in the proofs of asymptotic behavior.

1. The sampling locations will be expressed as $\mathbf{s}_i = L_n \mathbf{u}_i$, where $L_n \propto |\Omega_n|^{1/d}$ is the characteristic domain scale, and \mathbf{u}_i denote the realizations of the random vector $\mathbf{U}_i \supset [0, 1]^d$.

2. For any vectors $\mathbf{v}_i, \mathbf{v}_j$, the pair distance will be denoted by $\mathbf{v}_{i,j} := \mathbf{v}_i - \mathbf{v}_j$, and its Euclidean norm by $v_{i,j} := \|\mathbf{v}_i - \mathbf{v}_j\|$.
3. In integrals of kernel averages, the distance of the normalized sampling locations will be denoted by $\boldsymbol{\omega} := \mathbf{u}_i - \mathbf{u}_j$.
4. A vector $\boldsymbol{\omega}$ will be expressed in spherical polar coordinates as

$$\boldsymbol{\omega} = \omega \hat{\boldsymbol{\omega}} \quad \text{and} \quad (\hat{\boldsymbol{\omega}})_i = \cos \theta_i \prod_{0 \leq j < i} \sin \theta_j$$

where $\theta_0 = \pi/2$, $\theta_d = 0$, $\theta_{d-1} \in [0, 2\pi)$, and $\theta_i \in [0, \pi)$ for $i = 1, \dots, d-2$. The Jacobian of the transformation is given by $\omega^{d-1} J_d(\boldsymbol{\theta})$ where $\boldsymbol{\theta} = (\theta_1, \dots, \theta_{d-1})$ and

$$J_d(\boldsymbol{\theta}) = (\sin \theta_1)^{d-2} (\sin \theta_2)^{d-3} \dots \sin \theta_{d-2}.$$

The area of the d -dimensional unit sphere will be denoted by:

$$A_d := \int_{\mathbb{S}_d} d\boldsymbol{\theta} J_d(\boldsymbol{\theta}),$$

where $\int_{\mathbb{S}_d} := \int_0^\pi \dots \int_0^\pi \int_0^{2\pi}$.

5. The following aspect ratios will be used as small *perturbation parameters*: $p_n := h_1/L_n$ and $q_n := h_2/L_n$.

B. Conditions

The following conditions will be assumed to hold:

1. The normalized location random vectors $\mathbf{U}_1, \dots, \mathbf{U}_n$ are assumed to be independent and identically distributed.
2. The probability density function (pdf) $f_1(\mathbf{u}_{i,j})$ of the sampling-location pair-distance vector is continuously differentiable in a neighborhood of zero.

3. The joint pdfs $f_2(\mathbf{u}_{i,j}, \mathbf{u}_{i,k})$ and $f_3(\mathbf{u}_{i,j}, \mathbf{u}_{i,k}, \mathbf{u}_{i,l})$ are also continuously differentiable in a neighborhood of zero.
4. The conditional pdf $g_{\mathbf{u}}(\mathbf{u}_{i,j} | \mathbf{u}_j = \mathbf{u})$ is uniformly bounded in \mathbf{u} .
5. The joint moments of X^* are identical to those of X_λ . For example, $\forall \mathbf{s}_i, \mathbf{s}_j$, with $i \neq j$, $F^*(\mathbf{s}_i - \mathbf{s}_j) = F_\lambda(\mathbf{s}_i - \mathbf{s}_j)$.
6. The model semivariogram F_λ is continuous in a neighborhood of zero.
7. There exists a continuous and bounded function ψ_λ such that

$$\text{Cov} [(X_{i,j}^*)^2, (X_{p,q}^*)^2] = \psi_\lambda(s_{i,p}, s_{j,q}, s_{i,q}, s_{j,p}). \quad (30)$$

For example, if X_λ is a Gaussian SRF with semivariogram F_λ ,

$$\psi_\lambda(u_1, u_2, u_3, u_4) = 2 \left[F_\lambda(u_1) + F_\lambda(u_2) - F_\lambda(u_3) - F_\lambda(u_4) \right]^2.$$

8. If $\epsilon \ll 1$, there exist $c_1 \geq 1$ and three continuous functions g_1, g_2 and g_3 such that:

$$\psi_\lambda(0, 0, \epsilon s, \epsilon s) = g_1(s) \left(\frac{\epsilon}{\xi} \right)^{2c_1} + o \left(\frac{\epsilon}{\xi} \right)^{2c_1},$$

$$\psi_\lambda(\epsilon s_1, \epsilon s_2, 0, \epsilon s_3) = g_2(s_1, s_2, s_3) \left(\frac{\epsilon}{\xi} \right)^{2c_1} + o \left(\frac{\epsilon}{\xi} \right)^{2c_1}$$

and

$$\psi_\lambda \left(u_3, \left\| \epsilon \boldsymbol{\omega}_2 + u_3 \hat{\boldsymbol{\omega}}_3 - \epsilon \boldsymbol{\omega}_1 \right\|, \left\| u_3 \hat{\boldsymbol{\omega}}_3 + \epsilon \boldsymbol{\omega}_2 \right\|, \left\| u_3 \hat{\boldsymbol{\omega}}_3 - \epsilon \boldsymbol{\omega}_1 \right\| \right) = g_3(u_3, \boldsymbol{\omega}_1, \boldsymbol{\omega}_2, \boldsymbol{\theta}_1, \boldsymbol{\theta}_2, \boldsymbol{\theta}_3) \left(\frac{\epsilon}{\xi} \right)^{2c_1} + o \left(\frac{\epsilon}{\xi} \right)^{2c_1}.$$

For example, if X_λ is a Gaussian SRF with a spherical or exponential covariance function, the above conditions hold with $c_1 = 1$. In the case of differentiable covariance models commonly used (Gaussian, hole-type, rational quadratic, Cauchy) one has $c_1 = 2$.

9. The following integral of the function g_3 is bounded:
10. The bandwidths h_1 and h_2 tend to 0 as n tends to ∞ .
11. At the asymptotic limit, $|\Omega_n|/n$, tends to 0 as n tends to ∞ . This condition is satisfied simultaneously with $1/|\Omega_n| \rightarrow 0$, if $|\Omega_n| \propto n^\delta$ and $0 < \delta < 1$.

Conditions (1)-(4) specify properties of the sampling point distribution. Condition (5) expresses the correspondence between the SRF model and the sampled data. Conditions (6)-(9) specify properties which are satisfied by default for FGC-SSRFs. They are explicitly stated here, because the convergence properties of the constraint estimators are proved for more general cases, including non-Gaussian SRF models. In particular, conditions (7)-(9) are used in the analysis of the sample constraints variance. Conditions (10)-(11) imply an *asymptotic densification* of the sampling network, since the area enclosed by the convex hull increases slower than the number of points. For regular grids, this condition is obtained if the spacing decreases as the number of nodes increases. The densification conditions are necessary for proving asymptotic convergence of the estimators.

Lemma 1 *If the above conditions hold, the following is true:*

$$\Pr\left(\lim_{n \rightarrow \infty} \mathbb{K}_{h_1}\{A_{i,j}\} = n^2 \mathbb{E}[W_{i,j} A_{i,j}]\right) = 1, \quad (31)$$

where the indices i, j refer to any pair of non-identical sampling points. Similarly, if the summation is over a weighted k -point ($k \in \mathbb{Z}$) non-diagonal function, the result is $\propto n^k$.

This ergodic result follows directly by applying the arguments in the proof of Theorem 3.1 in Hall *et al.* [8], which will not be repeated here. Equation (31) enables the calculation of sample kernel averages in the asymptotic limit.

We will also use the following lemma:

Lemma 2 *Let X_n be a sequence of uniformly bounded random variables such that $X_n = o(1)$ almost surely. Then $\mathbb{E}[X_n]^k = o(1)$, for any k .*

C. Generalized Gradient Estimation

In this section we prove a relation between the “gradient” step and the kernel bandwidth h_1 , and we propose a physical estimate for the step. We also investigate the asymptotic properties of the mean and variance of the generalized gradient estimator.

Lemma 3 *The following relation holds between the bandwidth h_1 and the gradient step a_1 :*

$$a_1 = h_1 B_2^{1/2} + O(h_1 p_n) \quad \text{a.s.}, \quad (32)$$

where B_2 , is the kernel moment ratio defined in (19).

Proof:

Based on the consistency principle (25), the step a_1 is expressed as follows:

$$a_1^2 = \frac{\sum'_{i,j} W_{i,j} s_{i,j}^2}{\sum'_{i,j} W_{i,j}}. \quad (33)$$

The above can be calculated explicitly in the asymptotic regime using Lemma (1).

Leading-order calculation of $\mathbb{E}[W_{i,j}]$.

$$\mathbb{E}[W_{i,j}] = \int d\boldsymbol{\omega} K(L_n \|\boldsymbol{\omega}\|/h_1) f_1(\boldsymbol{\omega}).$$

The dominant asymptotic contribution from the integral is evaluated by means of a Taylor expansion of the pdf f_1 in terms of the small parameter p_n using the condition (2), i.e.,

$$\begin{aligned} \mathbb{E}[W_{i,j}] &= \int_0^\infty d\omega \omega^{d-1} K(\omega/p_n) \int_{\mathbb{S}_d} d\boldsymbol{\theta} J_d(\boldsymbol{\theta}) f_1(\omega \hat{\boldsymbol{\omega}}) \\ &= p_n^d \int_0^R du u^{d-1} K(u) \int_{\mathbb{S}_d} d\boldsymbol{\theta} J_d(\boldsymbol{\theta}) f_1(p_n u \hat{\boldsymbol{\omega}}) \\ &= p_n^d A_d f_1(0) m_{K,d} + O(p_n^{d+1}). \end{aligned} \quad (34)$$

This expansion gives the asymptotically dominant term of $\mathbb{E}[W_{i,j}]$. Based on Lemma (1) it follows that:

$$\sum'_{i,j} W_{i,j} = n^2 p_n^d A_d f_1(0) m_{K,d} + O(n^2 p_n^{d+1}) \quad \text{a.s.}, \quad (35)$$

where A_d is the area of the d -dimensional unit sphere defined in paragraph (4) of the Notation subsection.

Leading-order calculation of $\mathbb{E} [W_{i,j} s_{i,j}^2]$.

$$\begin{aligned} \mathbb{E} [W_{i,j} s_{i,j}^2] &= L_n^2 \mathbb{E} [s_{i,j}^2 K(p_n U_{i,j})] = L_n^2 \int d\boldsymbol{\omega} \|\boldsymbol{\omega}\|^2 K(\|\boldsymbol{\omega}\|/p_n) f_1(\boldsymbol{\omega}) \\ &= L_n^2 p_n^{d+2} A_d f_1(0) m_{K,d+2} + O(L_n^2 p_n^{d+3}). \end{aligned} \quad (36)$$

Hence, from Lemma (1) and equation (36) it follows that

$$\sum'_{i,j} W_{i,j} s_{i,j}^2 = n^2 L_n^2 p_n^{d+2} A_d f_1(0) m_{K,d+2} + O(n^2 L_n^2 p_n^{d+3}) \quad \text{a.s.} \quad (37)$$

Based on (33), (35), and (37) the asymptotic behavior of the step a_1 is given by:

$$a_1^2 = h_1^2 B_2 + O(h_1^2 p_n), \quad \text{a.s.}$$

1. Selection of Distance Step

Lemma (3) is valid for any step a_1 . We define by \mathfrak{B}_0 the set that includes for every sampling point \mathbf{s}_i the distance vectors from all its near neighbors \mathbf{s}_j , and also $N_0 = |\mathfrak{B}_0|$. A sensible estimate \hat{a}_1 is the geostatistical d -power average of the Euclidean distances, $\Delta_p \equiv \|\mathbf{s}_i - \mathbf{s}_j\|$, of all the vectors in \mathfrak{B}_0 i.e.,

$$\hat{a}_1^d = \frac{1}{N_0} \sum_{p=1}^{N_0} \Delta_p^d, \quad (38)$$

This definition implies that \hat{a}_1 is a random variable that depends on the sampling point configuration. In connection with the consistency principle, the bandwidth h_1 is also a random variable. However, since \hat{a}_1 represents an average over all the near neighbor distances for all the points, its fluctuations are not very significant. In particular, the coefficient of variation declines with the number of sample points. To avoid cumbersome notation we will not distinguish between h_1^m and \hat{a}_1^m , $m \in \mathbb{Z}^+$ and the respective stochastic moments in the following theorems on the asymptotic properties.

Remark 2 Other estimators of the distance step such as the median or the root mean square neighbor distances can be used. However, the equation (38) leads to consistent convergence properties for the variance of the sample constraints, regardless of the spatial dimension.

The kernel bandwidth, $\hat{h}_1 := h_1(\hat{a}_1)$, is then given in view of (32) by

$$\hat{h}_1 = \hat{a}_1 B_2^{-1/2}. \quad (39)$$

The above gives an explicit linear solution for the bandwidth in terms of the step. In practical applications p_n is a small parameter, and (39) is sufficient. Alternatively, (25) can be solved numerically to obtain the bandwidth in the pre-asymptotic case.

Lemma 4 *Let us assume that the sampling network densification conditions (10) and (11) hold, i.e., $|\Omega_n| \propto n^\delta$, where $0 < \delta < 1$ and $h_1 \propto n^{-\gamma}$ for every realization of the sampling network. Then, if the gradient step is defined by the equation (38), the bandwidth exponent satisfies the inequality $0 < \gamma \leq (1 - \delta)/d$.*

Proof: It holds that $\sum_{p=1}^{N_0} \Delta_p^d \geq v_d |\Omega_n|$ (where v_d is a geometric constant that depends on d). Since $N_0 > n$, in light of equations (38) and (39) it follows that $\hat{h}_1^d > v'_{1,d} n^{-(1-\delta)}$ for any n , which implies that $d\gamma \leq 1 - \delta$.

Theorem 1 (Mean of the Sample Gradient Constraint - Differentiable Case.) *Assume that conditions (1)-(11) above are satisfied, and that F_λ is four times differentiable in a neighborhood of zero. Then $\overline{\varphi}_1(h_1)$ is an asymptotically unbiased estimator of the stochastic constraint $\phi_1(a_1)$. More specifically, the following holds*

$$\mathbb{E}[\overline{\varphi}_1(h_1) - \phi_1(a_1)] = d\tau_2 h_1^4 (B_4 - B_2^2) + O(h_1^2 p_n) + o(h_1^4), \quad (40)$$

where $\tau_2 = F_\lambda^{(2)}(0)/2$.

Proof: Since $\overline{\varphi}_1(h_1) = d\overline{f}_X(h_1)$ and $\phi_1(a_1) = dF_\lambda(a_1)$ we focus on $\overline{f}_X(h_1)$ and F_λ to avoid unnecessary clutter. The sample function $\overline{f}_X(h_1)$, defined in (23), is expressed as follows in light of equations (20) and (22) :

$$\overline{f}_X(h_1) = \frac{\sum'_{i,j} W_{i,j} (X_{i,j}^*)^2}{2 \sum'_{i,j} W_{i,j}}. \quad (41)$$

$\mathbb{E}[\overline{f}_X(h_1)]$ involves an expectation over both the sampling point distribution and the distribution of the field values. Hence, we can write

$$\mathbb{E}[\overline{f}_X(h_1)] = \mathbb{E} \left\{ \mathbb{E} \left[\overline{f}_X(h_1) / \mathbf{U}_1, \dots, \mathbf{U}_n \right] \right\},$$

where the inner (conditional) expectation is over the field values keeping the sampling locations fixed, whereas the outer expectation is with respect to the sampling point distribution.

Calculation of the Conditional Expectation $\mathbb{E} [\overline{f_X}(h_1)/\mathbf{U}_1, \dots, \mathbf{U}_n]$.

Since only the numerator of (41) depends on the field values, we obtain

$$\mathbb{E} [\overline{f_X}(h_1)/\mathbf{U}_1, \dots, \mathbf{U}_n] = \frac{\mathbb{K}_{h_1} \left\{ F_\lambda(L_n \mathbf{U}_{i,j}) \right\}}{\mathbb{K}_{h_1} \{1\}}. \quad (42)$$

Leading-order calculation of $\mathbb{K}_{h_1} \left\{ F_\lambda(L_n \mathbf{U}_{i,j}) \right\}$.

Using Lemma (1) we obtain

$$\begin{aligned} \mathbb{E} \left[W_{i,j} \left\{ F_\lambda(L_n \mathbf{U}_{i,j}) \right\} \right] &= \int d\boldsymbol{\omega} K(\|\boldsymbol{\omega}\|/p_n) F_\lambda(L_n \|\boldsymbol{\omega}\|) f_1(\boldsymbol{\omega}) \\ &= \int d\omega \omega^{d-1} K(\omega/p_n) F_\lambda(L_n \omega) \int_{\mathbb{S}_d} d\boldsymbol{\theta} J_d(\boldsymbol{\theta}) f_1(\omega \hat{\boldsymbol{\omega}}) \\ &= p_n^d A_d [f_1(0) + O(p_n)] \int du u^{d-1} K(u) F_\lambda(h_1 u). \end{aligned}$$

Since the kernel is compactly supported, it is possible to approximate $F_\lambda(h_1 u)$ with a Taylor series expansion around zero, i.e.,

$$F_\lambda(h_1 u) = \tau_2 u^2 h_1^2 + \tau_4 u^4 h_1^4 + o(h_1^4), \quad (43)$$

where $\tau_i = F_\lambda^{(i)}(0)/i!$, $i = 2, 4$. Inserting the expansion in the integral it follows that

$$\mathbb{E} \left[W_{i,j} \left\{ F_\lambda(L_n \mathbf{U}_{i,j}) \right\} \right] = p_n^d A_d [f_1(0) + O(p_n)] \left[\tau_2 h_1^2 m_{K,d+2} + \tau_4 h_1^4 m_{K,d+4} + o(h_1^4) \right].$$

Finally, based on the above and Lemma (1), it follows that

$$\mathbb{K}_{h_1} \left\{ F_\lambda(L_n \mathbf{U}_{i,j}) \right\} = n^2 p_n^d A_d [f_1(0) + O(p_n)] \left[\tau_2 h_1^2 m_{K,d+2} + \tau_4 h_1^4 m_{K,d+4} + o(h_1^4) \right] \quad \text{a.s.}$$

Using this equation in connection with (35) and (41) leads to

$$\mathbb{E} [\overline{f_X}(h_1)/\mathbf{U}_1, \dots, \mathbf{U}_n] = \tau_2 h_1^2 B_2 + \tau_4 h_1^4 B_4 + O(h_1^2 p_n) + o(h_1^4) \quad \text{a.s.} \quad (44)$$

The respective expansion for $F_\lambda(a_1)$ is obtained using the consistency principle, (32), as well as equations (43) and (39), i.e.,

$$F_\lambda(a_1) = \tau_2 h_1^2 B_2 + \tau_4 h_1^4 B_2^2 + O(h_1^2 p_n) + o(h_1^4), \quad \text{a.s.} \quad (45)$$

From the equations (44), (45) and Lemma (2), it follows that

$$\mathbb{E} [\overline{f_X}(h_1) - F_\lambda(a_1)] = \tau_4 h_1^4 (B_4 - B_2^2) + O(h_1^2 p_n) + o(h_1^4). \quad (46)$$

The asymptotic convergence then follows from the densification effect, i.e., from $\gamma > 0$. In light of the above, $\overline{f_X}(h_1)$ is an asymptotically unbiased estimator of $F_\lambda(a_1)$, since the difference $\mathbb{E} [\overline{f_X}(h_1)] - F_\lambda(a_1)$ converges to 0 faster than each component as $h_1 \rightarrow 0$.

If we consider fluctuations in the bandwidth and the step, h_1 on the right hand-side of equation (46) should be replaced by the respective mean value, and the corrections should also include bandwidth fluctuations.

Remark 3 The asymptotic decline of the bias as h_1^4 follows from the consistency principle and does not require the specific choice of the step (38). The latter may only influence the upper bound of the bandwidth exponent γ .

The following is also a direct consequence of Theorem (1) and Lemma (3):

$$\mathbb{E}[\overline{\mathcal{S}}_1(a_1)] - \mathbb{E}[S_1(a_1)] = \tau_4 h_1^2 \left(\frac{B_4}{B_2} - B_2 \right) + O(p_n) + o(h_1^2). \quad (47)$$

Equation (47) shows that the generalized gradient $\overline{\mathcal{S}}_1(a_1)$ is an asymptotically unbiased estimator of the stochastic constraint $\mathbb{E}[S_1(a_1)]$.

Theorem 2 (Mean of the Sample “Gradient” Constraint - Continuous Case.) *Assume that conditions (1)-(11) above are satisfied, and that F_λ is continuous but non differentiable at zero. For $a'_1 = h_1 B_1$, it follows that $\overline{\varphi}_1(h_1)$ is an asymptotically unbiased estimator of the stochastic constraint $\phi_1(a'_1)$. More specifically:*

$$\mathbb{E}[\overline{\varphi}_1(h_1) - \phi_1(a'_1)] = d \tau_2 h_1^2 (B_2 - B_1^2) + d \tau_3 h_1^3 (B_3 - B_1^3) + O(h_1 p_n) + o(h_1^3). \quad (48)$$

In addition, $\overline{\varphi}_1(h_1)$ is an asymptotically biased estimator of the stochastic constraint $\phi_1(a_1)$, i.e.,

$$\mathbb{E}[\overline{\varphi}_1(h_1) - \phi_1(a_1)] = d \tau_1 h_1 (B_1 - B_2^{1/2}) + d \tau_3 h_1^3 (B_3 - B_2^{3/2}) + O(h_1 p_n) + o(h_1^3). \quad (49)$$

The mean relative error of $\mathbb{E}[\overline{\varphi}_1(h_1)]$ is given by

$$\psi_{\epsilon,1} := \mathbb{E} \left[\frac{\overline{\varphi}_1(h_1) - \phi_1(a_1)}{\phi_1(a_1)} \right] = \frac{B_{1,2}}{\sqrt{B_2}} + h_1^2 \frac{\tau_3}{\tau_1} \frac{B_{3,2}}{\sqrt{B_2}} + O(p_n) + o(h_1^2), \quad (50)$$

where $B_{1,2} = B_1 - B_2^{1/2}$, and $B_{3,2} = B_3 - B_2^{3/2}$.

Proof: The logic of the proof is the same as in Theorem (1), and therefore we only present the main points. The derivatives of F_λ do not exist at zero. However, if F_λ admits at least third-order derivatives for any $h_1 u > 0$, the Taylor series expansion of the semivariogram is expressed as

$$F_\lambda(h_1 u) = \tau_1 u h_1 + \tau_2 u^2 h_1^2 + \tau_3 u^3 h_1^3 + O(h_1 p_n) + o(h_1^3), \quad (51)$$

where $\tau_i = F_\lambda^{(i)}(0+)/i!$. Then we obtain

$$\mathbb{E} \left[W_{i,j} \left\{ F_\lambda(L_n \mathbf{U}_{i,j}) \right\} \right] = p_n^d A_d [f_1(0) + O(p_n)] \left[\sum_{j=1}^3 \tau_j h^j m_{K,d+j} + o(h_1^3) \right],$$

and in connection with (35) and (41) it follows that

$$\mathbb{E} [\overline{f_X}(h_1)/\mathbf{U}_1, \dots, \mathbf{U}_n] = \sum_{j=1}^3 \tau_j h^j B_j + o(h_1^3) \quad \text{a.s.} \quad (52)$$

Based on (51), the semivariogram $F_\lambda(a'_1)$ is expressed as

$$F_\lambda(a'_1) = \sum_{j=1}^3 \tau_j h^j B_1^j + O(h_1 p_n) + o(h_1^3). \quad (53)$$

Hence, we obtain

$$\mathbb{E} [\overline{f_X}(h_1)/\mathbf{U}_1, \dots, \mathbf{U}_n] - F_\lambda(a'_1) = \sum_{j=2,3} \tau_j h_1^j (B_j - B_1^j) + O(h_1 p_n) + o(h_1^3) \quad \text{a.s.} \quad (54)$$

The above proves equation (48). The equation (49) is proved in the same way, but the expansion (51) is replaced with an expansion around a_1 , i.e.,

$$F_\lambda(a_1) = \tau_1 h_1 B_2^{1/2} + \tau_2 h_1^2 B_2 + \tau_3 h_1^3 B_2^{3/2} + o(h_1^3). \quad (55)$$

The above, in connection with (52), leads to

$$\mathbb{E} [\overline{f_X}(h_1)/\mathbf{U}_1, \dots, \mathbf{U}_n] - F_\lambda(a_1) = \sum_{j=1,3} \tau_j h_1^j (B_j - B_2^{j/2}) + O(h_1 p_n) + o(h_1^3) \quad \text{a.s.} \quad (56)$$

Finally, equation (50) for the mean relative error (relative bias), follows from (55) and (56).

Based on equation (50) the relative bias depends on the kernel function through the coefficients $B_{1,2}$ and $B_{3,2}$. As $h_1 \rightarrow 0$, the relative bias converges to $B_{1,2}/B_2^{1/2}$.

Lemma 5 *The asymptotic relative bias, $\psi_{\epsilon,1}$, is a non-positive number.*

Proof: B_2 is a positive number. By definition, $B_{1,2} = B_1 - B_2^{1/2}$. Let us define the density function

$$f_K(s) := \frac{K(s) s^{d-1}}{\int_0^R K(s) s^{d-1}}, \quad s \in [0, R].$$

In light of this definition and equation (19), we obtain $B_m = \mathbb{E}_K[s^m]$, where E_K denotes the expectation with respect to the density function f_K . Then, $B_2 - B_1^2 = \mathbb{E}_K[(s - \mathbb{E}_K[s])^2] \geq 0$, and thus $B_{1,2} \leq 0$ follows directly.

As a direct consequence of equations (39) and (52), one obtains that $\mathbb{E}[\overline{\mathcal{S}}_1(a_1)] \propto O(h_1^{-1})$. Hence, the sample function $\overline{\mathcal{S}}_1(a_1)$ is not well defined at the asymptotic limit. Thus, the ‘‘gradient’’ constraints in the continuous but non-differentiable case refer to the sample function $\overline{\varphi}_1(h_1)$ and its stochastic counterpart, $\phi_1(a_1)$.

Theorem 3 (Variance of the Sample ‘‘Gradient’’ Constraint.) *If the conditions (1)-(11) above are satisfied, $\overline{\varphi}_1(h_1)$ is an asymptotically consistent estimator of $\phi_1(a_1)$. In particular, the variance of $\overline{\varphi}_1(h_1)$ is given asymptotically by:*

$$\text{Var}[\overline{\varphi}_1(h_1)] = O\left(\frac{1}{n^{2\epsilon_1\gamma+\epsilon_1}}\right), \quad \epsilon_1 = \min\{\delta, 2 - \delta - d\gamma\}. \quad (57)$$

Proof: The variance of $\overline{f}_X(h_1)$ is given by means of:

$$\text{Var}[\overline{f}_X(h_1)] = \mathbb{E}\left[\text{Var}[\overline{f}_X(h_1)/\mathbf{U}_1, \dots, \mathbf{U}_n]\right] + \text{Var}\left[\mathbb{E}[\overline{f}_X(h_1)/\mathbf{U}_1, \dots, \mathbf{U}_n]\right]. \quad (58)$$

According to Eq. (44) in the differentiable case, and Eq. (52) in the non-differentiable case, the second term on the right hand side of Eq. (58) is $o(h_1^2)$. Hence, we focus on the first term, which is expressed as follows:

$$\begin{aligned} \text{Var}[\overline{f}_X(h_1)/\mathbf{U}_1, \dots, \mathbf{U}_n] &= \sum'_{i,j} \sum'_{k,l} \frac{W_{i,j} W_{k,l}}{[\mathbb{K}_{h_1}(1)]^2} \text{Cov}\{(X_{i,j}^*)^2, (X_{k,l}^*)^2\} \\ &= V_{1,1} + V_{1,2} + V_{1,3}, \end{aligned} \quad (59)$$

where the functions $V_{1,1}, V_{1,2}, V_{1,3}$, in light of ψ_λ defined in (30), are given by

$$V_{1,1} = 2 \frac{\sum'_{i,j} W_{i,j}^2 \psi_\lambda(0, 0, s_{i,j}, s_{i,j})}{\left[\sum'_{i,j} W_{i,j}\right]^2} \quad (60)$$

$$V_{1,2} = 4 \frac{\sum'_{i,j,k} W_{i,j} W_{k,i} \psi_\lambda(s_{i,k}, s_{j,i}, 0, s_{j,k})}{\left[\sum'_{i,j} W_{i,j}\right]^2} \quad (61)$$

$$V_{1,3} = \frac{\sum'_{i,j,k,l} W_{i,j} W_{k,l} \psi_\lambda(s_{i,k}, s_{j,l}, s_{i,l}, s_{j,k})}{\left[\sum'_{i,j} W_{i,j}\right]^2}. \quad (62)$$

Leading-order calculation of the denominator.

The quantities $V_{1,1}, V_{1,2}, V_{1,3}$ in equations (60)-(62) have a common denominator, the asymptotic behavior of which follows from (35). More precisely, the following is true:

$$\left[\sum'_{i,j} W_{i,j}\right]^2 = n^4 p_n^{2d} [A_d f_1(0) m_{K,d}]^2 + o(n^4 p_n^{2d}) \quad \text{a.s.} \quad (63)$$

Leading-order calculation of $V_{1,1}$.

Denote the numerators of (60)-(62) by $N_{1,j}^{(v)}, j = 1, 2, 3$. Then, it follows from Lemma (1) that $N_{1,1}^{(v)} = 2n^2 \tilde{N}_{1,1}^{(v)}$ almost surely, where :

$$\begin{aligned} \tilde{N}_{1,1}^{(v)} &:= \mathbb{E} \left[W_{i,j}^2 \psi_\lambda(0, 0, L_n U_{i,j}, L_n U_{i,j}) \right] \\ &= \int d\boldsymbol{\omega} K^2(\|\boldsymbol{\omega}\|/p_n) \psi_\lambda(0, 0, L_n \|\boldsymbol{\omega}\|, L_n \|\boldsymbol{\omega}\|) f_1(\boldsymbol{\omega}). \end{aligned}$$

We use the variable $u = \omega/p_n$, and a Taylor expansion of f_1 around zero. We evaluate the integral over u with the mean value theorem. Finally, we apply the first scaling property of ψ_λ in condition (8), to obtain the following

$$\begin{aligned} \tilde{N}_{1,1}^{(v)} &= p_n^d \int du u^{d-1} K^2(u) \psi_\lambda(0, 0, uh_1, uh_1) \int_{\mathbb{S}_d} d\boldsymbol{\theta} J_d(\boldsymbol{\theta}) \left[f_1(0) + o(1) \right] \\ &= p_n^d g_1(u^*) \left(\frac{h_1}{\xi} \right)^{2c_1} A_d f_1(0) \int_0^R du u^{d-1} K^2(u) + o(p_n^d h_1^{2c_1}). \end{aligned}$$

Hence, it follows that $N_{1,1}^{(v)}$ is given by

$$N_{1,1}^{(v)} = 2 n^2 p_n^d g_1(u^*) \left(\frac{h_1}{\xi} \right)^{2c_1} A_d f_1(0) m_{K,d}^{(2)} + o(n^2 p_n^d h_1^{2c_1}) \quad \text{a.s.} \quad (64)$$

Finally, from equations (35), (63), (64) and based on Lemma (1), it follows that

$$V_{1,1} = \frac{2 g_1(u^*)}{A_d f_1(0) \xi^{2c_1}} \frac{m_{K,d}^{(2)}}{(m_{K,d})^2} \left(\frac{L_n^d}{n^2 h_1^{d-2c_1}} \right) + o\left(\frac{L_n^d}{n^2 h_1^{d-2c_1}} \right) \quad \text{a.s.} \quad (65)$$

Hence, the asymptotic dependence of $V_{1,1}$ on n becomes

$$V_{1,1} = O(n^{\delta-2+\gamma d-2c_1 \gamma}). \quad (66)$$

Leading-order calculation of $V_{1,2}$.

The numerator of $V_{1,2}$ is equal to $N_{1,2}^{(v)} = 4n^3 \tilde{N}_{1,2}^{(v)}$ almost surely, where:

$$\begin{aligned} \tilde{N}_{1,2}^{(v)} &:= \mathbb{E} \left[K(U_{i,j}/p_n) K(U_{i,k}/p_n) \psi_\lambda(L_n U_{i,k}, L_n U_{i,j}, 0, L_n U_{j,k}) \right] \\ &= \iint d\boldsymbol{\omega}_1 d\boldsymbol{\omega}_2 K\left(\frac{\|\boldsymbol{\omega}_1\|}{p_n}\right) K\left(\frac{\|\boldsymbol{\omega}_2\|}{p_n}\right) \psi_\lambda\left(L_n \|\boldsymbol{\omega}_2\|, L_n \|\boldsymbol{\omega}_1\|, 0, L_n \|\boldsymbol{\omega}_{1,2}\|\right) f_2(\boldsymbol{\omega}_1, \boldsymbol{\omega}_2). \end{aligned}$$

Converting $\boldsymbol{\omega}_1$ and $\boldsymbol{\omega}_2$ to spherical polar coordinates, using the perturbation parameter p_n with the change of variables $u_1 = \omega_1/p_n$, $u_2 = \omega_2/p_n$ leads to:

$$\begin{aligned} \tilde{N}_{1,2}^{(v)} &= p_n^{2d} \int du_1 u_1^{d-1} K(u_1) \int du_2 u_2^{d-1} K(u_2) \prod_{i=1,2} \int_{\mathbb{S}_d} d\boldsymbol{\theta}_i J_d(\boldsymbol{\theta}_i) \\ &\quad \psi_\lambda\left(L_n \omega_2, L_n \omega_1, 0, L_n \|\omega_1 \hat{\boldsymbol{\omega}}_1 - \omega_2 \hat{\boldsymbol{\omega}}_2\|\right) f_2(\omega_1 \hat{\boldsymbol{\omega}}_1, \omega_2 \hat{\boldsymbol{\omega}}_2). \end{aligned}$$

We evaluate the integrals over $\boldsymbol{\omega}_1$ and $\boldsymbol{\omega}_2$ using the mean value theorem, defining $u_{1,2}^* := \|\omega_1^* \hat{\boldsymbol{\omega}}_1^* - \omega_2^* \hat{\boldsymbol{\omega}}_2^*\|$. By applying the second scaling property of condition (8) for ψ_λ , the following is obtained:

$$\begin{aligned} \tilde{N}_{1,2}^{(v)} &= \psi_\lambda(h_1 u_2, h_1 u_1, 0, h_1 \|u_1 \hat{\boldsymbol{\omega}}_1 - u_2 \hat{\boldsymbol{\omega}}_2\|) f_2(p_n u_1 \hat{\boldsymbol{\omega}}_1, p_n u_2 \hat{\boldsymbol{\omega}}_2) \\ &= g_2(u_2^*, u_1^*, 0, u_{1,2}^*) \left(\frac{h_1}{\xi}\right)^{2c_1} p_n^{2d} (m_{K,d} A_d)^2 f_2(0) + o(p_n^{2d} h_1^{2c_1}). \end{aligned}$$

Hence, the following expression is obtained for the numerator of $V_{1,2}$:

$$\begin{aligned} N_{1,2}^{(v)} &= 4n^3 p_n^{2d} m_{K,d}^2 A_d^2 f_2(0) g_2(u_2^*, u_1^*, 0, u_{1,2}^*) \left(\frac{h_1}{\xi}\right)^{2c_1} \\ &\quad + o(p_n^{2d} n^3 h_1^{2c_1}) \quad \text{a.s.} \end{aligned} \quad (67)$$

Finally, based on equations (35), (63), (67) and Lemma (1), the following asymptotic expression is obtained for $V_{1,2}$

$$V_{1,2} = \frac{4g_2(u_2^*, u_1^*, 0, u_{1,2}^*) f_2(0)}{\xi^{2c_1} f_1^2(0)} \left(\frac{h_1^{2c_1}}{n}\right) + o\left(\frac{h_1^{2c_1}}{n}\right) \quad \text{a.s.} \quad (68)$$

Therefore, the asymptotic dependence of $V_{1,2}$ on n becomes

$$V_{1,2} = O(n^{-1-2c_1 \gamma}). \quad (69)$$

Leading-order calculation of $V_{1,3}$.

The numerator of $V_{1,3}$, $N_{1,3}^{(v)}$, includes a summation over quartets of sampling points and thus involves the joint pdf of three independent distances $(\mathbf{U}_{i,j}, \mathbf{U}_{k,l}, \mathbf{U}_{i,k})$. For reasons of brevity, we denote $\mathbf{u}_{i,j} = \boldsymbol{\omega}_1$, $\mathbf{u}_{k,l} = \boldsymbol{\omega}_2$, and $\mathbf{u}_{i,k} = \boldsymbol{\omega}_3$; then $\mathbf{u}_{i,l} = \boldsymbol{\omega}_2 + \boldsymbol{\omega}_3$, and $\mathbf{u}_{j,l} = \boldsymbol{\omega}_2 + \boldsymbol{\omega}_3 - \boldsymbol{\omega}_1$; also $u_{i,l} = \|\boldsymbol{\omega}_2 + \boldsymbol{\omega}_3\|$ and $u_{j,l} = \|\boldsymbol{\omega}_2 + \boldsymbol{\omega}_3 - \boldsymbol{\omega}_1\|$.

According to Lemma (1), $N_{1,3}^{(v)} = n^4 \tilde{N}_{1,3}^{(v)}$ almost surely, where $\tilde{N}_{1,3}^{(v)}$ is given by

$$\begin{aligned} \tilde{N}_{1,3}^{(v)} &:= \mathbb{E} \left[K(U_{i,j}/p_n) K(U_{k,l}/p_n) \psi_\lambda(L_n U_{i,k}, L_n U_{j,l}, L_n U_{i,l}, L_n U_{j,k}) \right] \\ &= \iiint d\boldsymbol{\omega}_1 d\boldsymbol{\omega}_2 d\boldsymbol{\omega}_3 K\left(\frac{\|\boldsymbol{\omega}_1\|}{p_n}\right) K\left(\frac{\|\boldsymbol{\omega}_2\|}{p_n}\right) f_3(\boldsymbol{\omega}_1, \boldsymbol{\omega}_3, \boldsymbol{\omega}_2 + \boldsymbol{\omega}_3) \\ &\quad \psi_\lambda(L_n \boldsymbol{\omega}_3, L_n u_{j,l}, L_n u_{i,l}, L_n \boldsymbol{\omega}_{1,3}). \end{aligned}$$

Converting $\boldsymbol{\omega}_1$, $\boldsymbol{\omega}_2$ and $\boldsymbol{\omega}_3$ to spherical polar coordinates, the following expression is obtained:

$$\begin{aligned} \tilde{N}_{1,3}^{(v)} &= \prod_{i=1}^3 \int d\omega_i (\omega_1 \omega_2 \omega_3)^{d-1} K\left(\frac{\omega_1}{p_n}\right) K\left(\frac{\omega_2}{p_n}\right) \prod_{i=1}^3 \int_{\mathbb{S}_d} d\boldsymbol{\theta}_i J_d(\boldsymbol{\theta}_i) \\ &\quad \psi_\lambda(L_n \boldsymbol{\omega}_3, L_n u_{j,l}, L_n u_{i,l}, L_n \boldsymbol{\omega}_{1,3}) f_3(\omega_1 \hat{\boldsymbol{\omega}}_1, \omega_3 \hat{\boldsymbol{\omega}}_3, \omega_2 \hat{\boldsymbol{\omega}}_2 + \omega_3 \hat{\boldsymbol{\omega}}_3). \end{aligned}$$

Using the variable transformations $u_1 = \omega_1/p_n$, $u_2 = \omega_2/p_n$, $u_3 = L_n \omega_3$, and the Taylor expansion of f_3 around $(0, 0, 0)$, $N_{1,3}^{(v)}$ is transformed as follows

$$\begin{aligned} \tilde{N}_{1,3}^{(v)} &= \frac{p_n^{2d}}{L_n^d} \int du_1 \int du_2 \int du_3 (u_1 u_2 u_3)^{d-1} K(u_1) K(u_2) \prod_{i=1}^3 \int_{\mathbb{S}_d} d\boldsymbol{\theta}_i J_d(\boldsymbol{\theta}_i) \\ &\quad \psi_\lambda(u_3, \|h_1 u_2 \hat{\boldsymbol{\omega}}_2 + u_3 \hat{\boldsymbol{\omega}}_3 - h_1 u_1 \hat{\boldsymbol{\omega}}_1\|, \|u_3 \hat{\boldsymbol{\omega}}_3 + h_1 u_2 \hat{\boldsymbol{\omega}}_2\|, \\ &\quad \|u_3 \hat{\boldsymbol{\omega}}_3 - h_1 u_1 \hat{\boldsymbol{\omega}}_1\|) \left[f_3(0, 0, 0) + o(1) \right]. \end{aligned}$$

The integrals over u_1 , u_2 and $\boldsymbol{\theta}_i$ are evaluated using the mean value theorem and the third scaling property of condition (8):

$$\begin{aligned} \tilde{N}_{1,3}^{(v)} &= \frac{p_n^{2d}}{L_n^d} \left(\frac{h_1}{\xi}\right)^{2c_1} f_3(\mathbf{0}) \left(m_{K,d} A_d\right)^2 \int du_3 u_3^{d-1} g_3(u_3, u_1^*, u_2^*, \boldsymbol{\theta}_1^*, \boldsymbol{\theta}_2^*, \boldsymbol{\theta}_3^*) \\ &\quad + o(p_n^{2d} L_n^{-d} h_1^{2c_1}). \end{aligned}$$

Finally, the following expression is obtained for $N_{1,3}^{(v)}$

$$N_{1,3}^{(v)} = C^* n^4 \left(\frac{p_n^2}{L_n}\right)^d \left(\frac{h_1}{\xi}\right)^{2c_1} f_3(\mathbf{0}) (m_{K,d} A_d)^2 + o(p_n^{2d} L_n^{-d} h_1^{2c_1}), \quad (70)$$

where $C^* = \int du_3 u_3^{d-1} g_3(u_3, u_1^*, u_2^*, \boldsymbol{\theta}_1^*, \boldsymbol{\theta}_2^*, \boldsymbol{\theta}_3^*)$ is a finite constant thanks to assumption (9).

Hence, based on equations (37), (63), (70) and Lemma (1), the following asymptotic expression is obtained for $V_{1,3}$

$$V_{1,3} = \frac{C^* f_3(\mathbf{0})}{\xi^{2c_1} f_1^2(0)} \left(\frac{h_1^{2c_1}}{L_n^d} \right) + o\left(\frac{h_1^{2c_1}}{L_n^d} \right) \quad \text{a.s.} \quad (71)$$

Hence, the asymptotic dependence of $V_{1,3}$ on n becomes

$$V_{1,3} = O(n^{-\delta-2c_1\gamma}). \quad (72)$$

Variance Convergence Rate.

Based on equations (66), (69) and (72), the convergence of $V_{1,3}$ is slower than that of $V_{1,2}$ since $\delta < 1$. The convergence of $V_{1,1}$ is faster than that of $V_{1,3}$ if $\gamma d < 2(1 - \delta)$. If this condition holds, then $V_{1,3}$ is the rate-limiting term. In light of Lemma (4) this inequality is satisfied for the bandwidth defined by (38).

Remark 4 The rate of convergence of the gradient estimator's variance is the same for the differentiable and non-differentiable cases. The three terms, i.e., $V_{1,1}, V_{1,2}, V_{1,3}$, possess distinct convergence rates. These terms correspond to sample functions that involve doublets, triplets and quartets of non-identical sampling points. Using the step estimate (38) and the consistency principle, the slowest convergence rate (asymptotically dominant term) is due to the term that involves quartets of non-identical points. On intuitive grounds, we would expect the same behavior to hold for different step estimates.

D. Generalized Curvature Estimation

In this section we prove a relation between the ‘‘curvature’’ step and the kernel bandwidth h_2 , and we propose an estimate for the step. We then investigate the asymptotic properties of the mean and variance of the generalized curvature estimator. In the process, we also show that to a first approximation $\mu_1 = \mu_2 = 1$ and we calculate the asymptotic dependence of the leading corrections.

In the proofs of asymptotic dependence, we will use the following modification of Lemma (1).

$$\Pr\left(\lim_{n \rightarrow \infty} \mathbb{K}_{rh_2} \{A_{i,j}\} = n^2 \mathbb{E} [Q_{i,j(r)} A_{i,j}] \right) = 1. \quad (73)$$

Lemma 6 *The following relation holds between the bandwidth h_2 and the curvature step a_2 :*

$$a_2^4 = h_2^4 B_4 + O(h_2 q_n) \quad \text{a.s..}$$

Proof: The proof is along the lines of Lemma (3). According to the definition (29) and the kernel-average equation (22), the step a_2 is defined by:

$$a_2^4 := \langle s_{i,j}^4 \rangle_{h_2} = \frac{\mathbb{K}_{h_2} \{s_{i,j}^4\}}{\mathbb{K}_{h_2} \{1\}}. \quad (74)$$

Leading-order calculation of $\mathbb{E}[Q_{i,j(r)}]$.

$$\begin{aligned} \mathbb{E}[Q_{i,j(r)}] &= \int d\boldsymbol{\omega} K(L_n \|\boldsymbol{\omega}\| / r h_2) f_1(\boldsymbol{\omega}) \\ &= \int d\boldsymbol{\omega} \omega^{d-1} K(\omega / r q_n) \int_{\mathbb{S}_d} d\boldsymbol{\theta} J_d(\boldsymbol{\theta}) f_1(\omega \hat{\boldsymbol{\omega}}) \\ &= r^d q_n^d A_d f_1(0) m_{K,d} + O(q_n^{d+1}). \end{aligned} \quad (75)$$

Hence, we obtain

$$\mathbb{K}_{rh_2} \{1\} = n^2 r^d q_n^d A_d f_1(0) m_{K,d} + O(n^2 q_n^{d+1}) \quad \text{a.s..} \quad (76)$$

The term $\mathbb{K}_{h_2} \{s_{i,j}^4\}$ is a special case of $\mathbb{K}_{rh_2} \{s_{i,j}^m\}$, which we evaluate below.

Leading-order calculation of $\mathbb{E}[Q_{i,j(r)} s_{i,j}^m]$.

$$\begin{aligned} \mathbb{E}[Q_{i,j(r)} s_{i,j}^m] &= L_n^m \int d\boldsymbol{\omega} \|\boldsymbol{\omega}\|^m K(\|\boldsymbol{\omega}\| / r q_n) f_1(\boldsymbol{\omega}) \\ &= L_n^m r^{d+m} q_n^{d+m} A_d f_1(0) m_{K,d+m} + O(L_n^m q_n^{d+5}). \end{aligned}$$

Hence, it follows that

$$\mathbb{K}_{rh_2} \{s_{i,j}^m\} = n^2 L_n^m r^{d+m} q_n^{d+m} A_d f_1(0) m_{K,d+m} + O(n^2 q_n^{d+1+m}) \quad \text{a.s..} \quad (77)$$

From the Eqs. (76) and (77) it follows that

$$\langle s_{i,j}^m \rangle_{rh_2} \equiv \frac{\mathbb{K}_{rh_2} \{s_{i,j}^m\}}{\mathbb{K}_{rh_2} \{1\}} = r^m h_2^m B_m + O(h_2^m q_n) \quad \text{a.s..} \quad (78)$$

The asymptotic behavior of a_2 is obtained from (78) for $r = 1$ and $m = 4$:

$$a_2^4 = h_2^4 B_4 + O(h_2^4 q_n) \quad \text{a.s..} \quad (79)$$

The coefficients $\mu_1(h_1)$ and $\mu_2(h_2)$ appear in the definition of the generalized curvature constraint. We calculate the asymptotic dependence of these coefficients.

Lemma 7 *The coefficients $\mu_1(h_1)$ and $\mu_2(h_2)$ are given asymptotically by:*

$$\mu_j(h_j) = 1 + o(1) \quad \text{a.s., for } j = 1, 2.$$

Proof: Based on the equations (27) and (28) the coefficients involve the averages $\langle s_{i,j}^2 \rangle_{rh_2}$ and $\langle s_{i,j}^4 \rangle_{rh_2}$, where $r = 1, 2, \sqrt{2}$. Both averages are given by equation (78). The lemma is proved following straightforward but tedious algebraic manipulations.

For the curvature step we will use the same expression as for the gradient step, i.e., $\hat{a}_2 = \hat{a}_1$, given by equation (38). The kernel bandwidth, $\hat{h}_2 := h_2(\hat{a}_2)$, is then given in view of (79) as follows:

$$\hat{h}_2 = \hat{a}_2 B_4^{-1/4}. \quad (80)$$

Lemma 8 *Let us assume that $h_2 \propto n^{-\nu}$. Then, if the curvature step is defined by the equation (38), the bandwidth exponent satisfies the inequality $0 < \nu d \leq 1 - \delta$.*

Proof: The proof is completely analogous to the proof of Lemma (4) if γ is replaced by ν .

Theorem 4 (Mean of the Sample Curvature Constraint - Differentiable Case.) *Assume that hypotheses (1)-(11) above are satisfied, and that F_λ admits five derivatives in a neighborhood of zero. Then $\overline{\varphi}_2(h_2)$ is an asymptotically unbiased estimator of $\phi_2(a_2)$. More specifically, the following holds*

$$\mathbb{E} [\overline{\varphi}_2(h_2) - \phi_2(a_2)] = -24d(d+4) \tau_6 h_2^6 \left(B_6 - B_4^{3/2} \right) + O(h_2^2 q_n) + o(h_2^6), \quad (81)$$

where $\tau_6 =$ and $g_k = m_{K,d+k}/m_{K,d}$.

Proof:

Based on (26), $\phi_2(a_2)$ is expressed in terms of $\overline{f_X}(rh_2)$ as follows:

$$\overline{\varphi}_2(h_2) = \frac{1}{2} \left[c_d^{(2)} \mu_1(h_2) \overline{f_X}(h_2) - c_d^{(3)} \mu_2(h_2) \overline{f_X}(\sqrt{2}h_2) - c_d^{(1)} \overline{f_X}(2h_2) \right]. \quad (82)$$

The sample function $\overline{f_X}(rh_2)$ is defined in terms of (23), and it is expressed in light of (21) as follows:

$$\overline{f_X}(rh_2) = \frac{\sum'_{i,j} Q_{i,j(r)} (X_{i,j}^*)^2}{2 \sum'_{i,j} Q_{i,j}}. \quad (83)$$

Hence, $\mathbb{E}[\overline{\varphi_2}(h_2)]$ is expressed in terms of $\mathbb{E}[\overline{f_X}(rh_2)]$. As in Theorem (1), the ensemble average implies $\mathbb{E}[\overline{f_X}(rh_2)] = \mathbb{E} \left\{ \mathbb{E} \left[\overline{f_X}(rh_2) / \mathbf{U}_1, \dots, \mathbf{U}_n \right] \right\}$.

Calculation of the Conditional Expectation $\mathbb{E} \left[\overline{f_X}(rh_2) / \mathbf{U}_1, \dots, \mathbf{U}_n \right]$.

Only the numerator of (83) depends on the field values, i.e.,

$$\mathbb{E} \left[\overline{f_X}(rh_2) / \mathbf{U}_1, \dots, \mathbf{U}_n \right] = \frac{\mathbb{K}_{rh_2} \left\{ F_\lambda(L_n \mathbf{U}_{i,j}) \right\}}{\mathbb{K}_{rh_2} \{1\}}. \quad (84)$$

Leading-order calculation of $\mathbb{K}_{rh_2} \left\{ F_\lambda(L_n \mathbf{U}_{i,j}) \right\}$.

$$\begin{aligned} \mathbb{E} \left[Q_{i,j(r)} \left\{ F_\lambda(L_n \mathbf{U}_{i,j}) \right\} \right] &= \int d\boldsymbol{\omega} K(\|\boldsymbol{\omega}\|/(rq_n)) F_\lambda(L_n \|\boldsymbol{\omega}\|) f_1(\boldsymbol{\omega}) \\ &= \int d\omega \omega^{d-1} K(\omega/(rq_n)) F_\lambda(L_n \omega) \int_{\mathbb{S}_d} d\boldsymbol{\theta} J_d(\boldsymbol{\theta}) f_1(\omega \hat{\boldsymbol{\omega}}) \\ &= r^d q_n^d A_d [f_1(0) + O(p_n)] \int du u^{d-1} K(u) F_\lambda(r h_2 u). \end{aligned}$$

The sixth-order Taylor series expansion of $F_\lambda(r h_2 u)$ around zero yields

$$F_\lambda(r h_2 u) = \tau_2 r^2 u^2 h_2^2 + \tau_4 r^4 u^4 h_2^4 + \tau_6 r^6 h_2^6 + o(h_2^6). \quad (85)$$

Inserting the expansion in the kernel integral, it follows that

$$\mathbb{E} \left[Q_{i,j(r)} \left\{ F_\lambda(L_n \mathbf{U}_{i,j}) \right\} \right] = q_n^d A_d [f_1(0) + O(p_n)] \left[\sum_{i=2,4,6} m_{K,d+i} \tau_i (r h_2)^i + o(h_2^6) \right].$$

The above in connection with (76) for the kernel average $\mathbb{K}_{rh_2} \{1\}$ lead to:

$$\mathbb{E} \left[\overline{f_X}(rh_2) / \mathbf{U}_1, \dots, \mathbf{U}_n \right] = \sum_{i=2,4,6} g_i \tau_i (r h_2)^i + O(h_2^2 q_n) + o(h_2^6) \quad \text{a.s.} \quad (86)$$

From (86) and (82) it follows that the $O(h_2^2)$ term vanishes if the coefficients $\mu_1(h_1), \mu_2(h_2)$ are defined as in equations (27) and (28). Finally, we obtain

$$\mathbb{E} \left[\overline{\varphi_2}(h_2) / \mathbf{U}_1, \dots, \mathbf{U}_n \right] = -c_d^{(0)} B_4 \tau_4 h_2^4 - 24d(d+4) B_6 \tau_6 h_2^6 + O(h_2^2 q_n) + o(h_2^6) \quad \text{a.s.}$$

Using the definition of $\phi_2(a_2)$, equation (9), the expansion (85), and the step - bandwidth relation, (80), a series expansion is obtained for $\phi_2(a_2)$

$$\phi_2(a_2) = -c_d^{(0)} \tau_4 h_2^4 B_4 - 24d(d+4) \tau_6 h_2^6 B_4^{3/2} + O(h_2^2 q_n) + o(h_2^6), \quad \text{a.s..}$$

The two preceding expansions allow calculating the bias for the curvature constraint by subtracting the terms on the respective sides. The proof is completed by applying Lemma 2 to obtain equation (81).

Theorem 5 (Mean of the Sample ‘‘Curvature’’ Constraint - Continuous Case.) *Assume that conditions (1)-(11) above are satisfied, and that F_λ is continuous but non differentiable at zero. For $a'_2 = h_2 B_1$, it follows that $\overline{\varphi}_2(h_2)$ is an asymptotically unbiased estimator of the stochastic constraint $\phi_2(a'_2)$. More specifically, if $c_d^{(4)} = [c_d^{(2)} - \sqrt{2} c_d^{(3)} - 2c_d^{(1)}]$, and $c_d^{(5)} = [c_d^{(2)} - 2\sqrt{2} c_d^{(3)} - 8c_d^{(1)}]$ then:*

$$\mathbb{E} [\overline{\varphi}_2(h_2) - \phi_2(a'_2)] = c_d^{(5)} \tau_3 h_2^3 (B_3 - B_1^3) + o(h_2^3) + O(h_2 q_n). \quad (87)$$

In addition, $\overline{\varphi}_2(h_2)$ is an asymptotically biased estimator of the stochastic constraint $\phi_2(a_2)$, i.e.,

$$\begin{aligned} \mathbb{E} [\overline{\varphi}_2(h_2) - \phi_2(a_2)] &= c_d^{(4)} \tau_1 h_2 (B_1 - B_4^{1/4}) + c_d^{(5)} \tau_3 h_2^3 (B_3 - B_4^{3/4}) \\ &+ o(h_2^3) + O(h_2 q_n). \end{aligned} \quad (88)$$

The mean relative error of $\mathbb{E}[\overline{\varphi}_2(h_2)]$ is given by

$$\psi_{\epsilon,2} := \mathbb{E} \left[\frac{\overline{\varphi}_2(h_2) - \phi_2(a_2)}{\phi_2(a_2)} \right] = \frac{B_{1,4}}{B_4^{1/4}} + h_2^2 \left(\frac{\tau_3}{\tau_1} \right) \frac{B_{3,4}}{B_4^{1/4}} + O(p_n) + o(h_2^2), \quad (89)$$

where $B_{1,4} = B_1 - B_4^{1/4}$, and $B_{3,4} = B_3 - B_4^{3/4}$.

Proof:

First we calculate $\mathbb{E} [\overline{\varphi}_2(h_2)/\mathbf{U}_1, \dots, \mathbf{U}_n]$. This requires calculation of $\mathbb{E} [\overline{f}_X(rh_2)/\mathbf{U}_1, \dots, \mathbf{U}_n]$. The latter is given in equation (84). On the right hand side of that equation, the denominator, $\mathbb{K}_{rh_2}\{1\}$, is given by equation (76). The numerator, $\mathbb{K}_{rh_2}\{F_\lambda(L_n \mathbf{U}_{i,j})\}$, converges to $n^2 \mathbb{E} \left[Q_{i,j(r)} \left\{ F_\lambda(L_n \mathbf{U}_{i,j}) \right\} \right]$ according to (73).

For $h_2 u > 0$ the Taylor expansion of F_λ is given by

$$F_\lambda(r h_2 u) = \tau_1 r u h_2 + \tau_2 r^2 u^2 h_2^2 + \tau_3 r^3 u^3 h_2^3 + o(h_2^3). \quad (90)$$

where $\tau_i = F_\lambda^{(i)}(0^+)$. Then, we obtain by the standard procedure

$$\mathbb{E} \left[Q_{i,j(r)} \left\{ F_\lambda(L_n \mathbf{U}_{i,j}) \right\} \right] = q_n^d A_d [f_1(0) + O(q_n)] \left[\sum_{j=1}^3 \tau_j r^j h_2^j m_{K,d+j} + o(h_2^3) \right].$$

Based on the above, it follows that

$$\mathbb{E} [\overline{f}_X(rh_2)/\mathbf{U}_1, \dots, \mathbf{U}_n] = \sum_{j=1,2,3} \tau_j r^j h_2^j B_j + O(h_2 q_n) + o(h_2^3) \quad \text{a.s.} \quad (91)$$

Finally, using Lemma (2) and equation (82), we obtain the following

$$\mathbb{E} [\overline{\varphi}_2(h_2)/\mathbf{U}_1, \dots, \mathbf{U}_n] = c_d^{(4)} \tau_1 h_2 B_1 + c_d^{(5)} \tau_3 h_2^3 B_3 + o(h_2^3) + O(h_2 q_n) \quad \text{a.s.},$$

where the term $O(h_2^3)$ vanishes due to cancelation of the coefficients. Based on (9) and the expansion (90), the stochastic term is expressed as $\phi_2(a'_2 = B_1 h_2) = c_d^{(4)} \tau_1 h_2 B_1 + c_d^{(5)} \tau_3 h_2^3 B_1^3 + o(h_2^3)$. This expansion in connection with the one above for $\mathbb{E} [\overline{\varphi}_2(h_2)/\mathbf{U}_1, \dots, \mathbf{U}_n]$ leads to

$$\mathbb{E} [\overline{\varphi}_2(h_2)/\mathbf{U}_1, \dots, \mathbf{U}_n] - \phi_2(a'_2) = c_d^{(5)} \tau_3 h_2^3 (B_3 - B_1^3) + o(h_2^3) + O(h_2 q_n) \quad \text{a.s.}$$

The proof of equation (87) is completed by applying Lemma 2 to the above result. The estimator is asymptotically unbiased since the bias converges to 0 faster than either the sample or the stochastic constraints.

Equations (88) and (89) follow along the same lines. The main difference is that the stochastic constraint now becomes $\phi_2(a_2)$, where $a_2 = (B_4^{1/4}) h_2$ according to (80).

Lemma 9 *The asymptotic relative bias, $\psi_{\epsilon,2}$, is non-positive.*

Proof: As $h_2 \rightarrow 0$, the relative bias converges to $B_{1,4}/B_4^{1/4}$. B_4 is a positive number. By definition, $B_{1,4} = B_1 - B_4^{1/4}$. Using the density function defined in Lemma (5), we can write $B_4 - B_1^4 \geq \mathbb{E}_K \left[\{s^2 - \mathbb{E}_K^2[s]\}^2 \right] \geq 0$, from which it follows that $B_{1,4} \leq 0$.

Theorem 6 (Variance of the Sample ‘‘Curvature’’ Constraint.) *If the hypotheses (1)-(11) above are satisfied, then $\overline{\varphi}_2(h_2)$ is an asymptotically consistent estimator $\phi_2(a_2)$. More specifically, the following holds:*

$$\text{Var} [\overline{\varphi}_2(h_2)] = O \left(\frac{1}{n^{2c_1\nu+\epsilon_2}} \right), \quad \epsilon_2 = \min\{\delta, 2 - \delta - d\nu\}. \quad (92)$$

Proof: The proof is based on the same approach as in Theorem 3. The calculations are more extended due to the cross-products between the sample functions $\overline{f}_X(h_2)$, $\overline{f}_X(\sqrt{2}h_2)$ and $\overline{f}_X(2h_2)$. However, in this case we also obtain terms containing doublets, triplets and quartets of sampling points. Since the complications are of a trivial nature, the lengthy calculations will be omitted here. Using for the curvature step equation (38), the quartet term dominates the convergence. This term leads to the slow asymptotic decline of the variance as $O(h_2^{2c_1}/L_n^d)$ or equivalently as $O(n^{-2c_1\nu-\delta})$.

	Triangular	Quadratic	Gaussian	Tricube
$B_{1,2}$	-0.0472	-0.0440	-0.1138	-0.0390
B_2	1/5	1/3	1	22/91
$\psi_{\epsilon,1}$	-0.1056	-0.0762	-0.1138	-0.0793
$B_{1,4}$	-0.1170	-0.1056	-0.3030	-0.0959
B_4	1/14	1/6	2	22/243
$\psi_{\epsilon,2}$	-0.2263	-0.1653	-0.2548	0.1748

TABLE I: Calculations of $B_{1,2}$, $B_{1,4}$, B_2 , B_4 , and the relative bias of the “gradient” and “curvature” constraint estimators using different kernel functions.

E. Calculation of Asymptotic Bias

The asymptotic relative bias of the “gradient” and “curvature” constraint estimators obtained for different types of kernel functions, according to equations (50) and (89), is shown in Table (I). In particular, we include the *Gaussian kernel*, $K(s) = \exp(-s^2)$, the *triangular kernel*, $K(s) = (1 - \|s\|) \mathbb{1}_{0 \leq \|s\| \leq 1}$, the *quadratic kernel*, $K(s) = (1 - \|s\|^2) \mathbb{1}_{0 \leq \|s\| \leq 1}$, and the *tricube kernel*, $K(s) = (1 - \|s\|^3)^3 \mathbb{1}_{0 \leq \|s\| \leq 1}$. The Gaussian kernel is not compactly supported, but it decays to zero very fast. The quadratic kernel gives the lowest relative bias, followed by the tricube kernel.

VII. SSRF MODEL PARAMETER INFERENCE

Model parameter inference is based on the procedure introduced in [12], which is expanded herein. The main idea is to estimate the SSRF parameters, θ by matching sample constraints with their stochastic counterparts. We use the sample constraints $\overline{\mathcal{S}}_0$, $\overline{\mathcal{S}}_1(\hat{a}_1)$ and $\overline{\mathcal{S}}_2(\hat{a}_2)$, given by equations (16), (24), (26) respectively, as well as the stochastic constraints $\mathbb{E}[S_0]$, $\mathbb{E}[S_1(\hat{a}_1)]$ and $\mathbb{E}[S_2(\hat{a}_2)]$, given by equations (11), (14), (15) respectively. We also impose the normalization constraint (13).

Determining θ is then expressed as an optimization problem that aims at minimizing the deviation between the stochastic moments and their estimators; the latter include the sample-based variance, gradient, and curvature constraints, and 1 for the normalization

constraint. We introduce the metric $\Phi(\mathbf{X}^*; \boldsymbol{\theta}')$ to measure the distance between the sample and ensemble constraints:

$$\begin{aligned} \Phi(\mathbf{X}^*; \boldsymbol{\theta}') := & \left\{ 1 - (S'_0)^{1/\beta} \right\}^2 + \left\{ 1 - \left(\frac{\overline{\mathcal{S}}_0}{\overline{\mathcal{S}}_1(\hat{a}_1)} \frac{\mathbb{E}[S_1(\hat{a}_1)]}{\mathbb{E}[S_0]} \right)^{1/\beta} \right\}^2 \\ & + \left\{ 1 - \left(\frac{\overline{\mathcal{S}}_1(\hat{a}_1) \mathbb{E}[S_2(\hat{a}_2)]}{\overline{\mathcal{S}}_2(\hat{a}_2) \mathbb{E}[S_1(\hat{a}_1)]} \right)^{1/\beta} \right\}^2 \end{aligned} \quad (93)$$

In equation (93), $\mathbb{E}[S_0]$, $\mathbb{E}[S_1(\hat{a}_1)]$ and $\mathbb{E}[S_2(\hat{a}_2)]$ are the values of the constraints obtained for the “current” values of the Spartan parameters η_1 , ξ and k_{\max} and for $\hat{a}_1 = \hat{a}_2$ as given by (38). The simplex search method of Nelder and Mead [21] is used for the optimization. The initial parameter vector $\boldsymbol{\theta}^{(0)}$ is updated at every optimization step. For η_1 the value $\eta_1^{(0)} = 1$ is arbitrarily chosen. The initial value $\xi^{(0)}$ of the characteristic length is estimated from the data. The initial estimate of the characteristic length is given by $\xi^{(0)} = [\overline{\mathcal{S}}_1(\hat{a}_1)/\overline{\mathcal{S}}_2(\hat{a}_2)]^{1/2}$. The frequency cutoff k_c is chosen according $k_c^{(0)} = 2\pi\hat{a}_1^{-1}$. The final vector, $\hat{\boldsymbol{\theta}}$, to which the optimization converges gives the optimal parameters of the SSRF model.

Note that the functional $\Phi(\mathbf{X}^*; \boldsymbol{\theta}')$ is independent of η_0 , which can be set equal to 1 during the optimization. The optimal $\hat{\eta}_0$ is obtained using the condition of the variance independence from $k_c\xi$ and η_1 , i.e., equation (12), which leads to the following:

$$\hat{\eta}_0 = 2^d \pi^{d/2} \Gamma(d/2) \hat{\sigma}_x^2. \quad (94)$$

In light of (11) and (13), equation (94) guarantees that the model variance matches the sample variance.

Some comments are in order regarding the definition of the distance metric (93). The functional is of the general form $\Phi = \sum_{i=1}^3 (1 - z_i^{1/\beta})^2$, where

$$z_1 = S'_0, \quad z_2 = \frac{\overline{\mathcal{S}}_0 \mathbb{E}[S_1(\hat{a}_1)]}{\overline{\mathcal{S}}_1(\hat{a}_1) \mathbb{E}[S_0]}, \quad z_3 = \frac{\overline{\mathcal{S}}_1(\hat{a}_1) \mathbb{E}[S_2(\hat{a}_2)]}{\overline{\mathcal{S}}_2(\hat{a}_2) \mathbb{E}[S_1(\hat{a}_1)]}.$$

The number of terms (squares) in Φ is equal to the number of variables. The z_i are functions that involve specific sample and ensemble constraints. The definitions of z_2 , z_3 are motivated by the goals of (i) eliminating the dependence on η_0 (since the latter is an overall scaling factor) (ii) defining dimensionless variables so that the optimization does not depend on the units used and (iii) forming combinations of constraints of similar magnitude so that they contribute on an equal footing in the optimization.

Straightforward constraint differences, i.e., $\overline{\mathcal{S}}_i - \mathbb{E}[S_i]$ are neither dimensionless nor of similar magnitude. Using ratios $\overline{\mathcal{S}}_i/\mathbb{E}[S_i]$ yields dimensionless ratios of similar magnitude, but it preserves the η_0 dependence. The proposed combinations for z_i for $i = 2, 3$, which are of the form $\overline{\mathcal{S}}_{i-1}\mathbb{E}[S_i]/\overline{\mathcal{S}}_i\mathbb{E}[S_{i-1}]$ involve ratios of the form $\mathbb{E}[S_i]/\mathbb{E}[S_{i-1}]$, which eliminate the η_0 dependence. A significant advantage of using ratios $\overline{\mathcal{S}}_i/\mathbb{E}[S_i]$ is that $\overline{\mathcal{S}}_i/\mathbb{E}[S_i] = \overline{\varphi_i(h_i)}/\phi_i(a_i)$ for $i = 1, 2$. That is, the terms a_i^{2i} in the denominators of both $\overline{\mathcal{S}}_i$ and $\mathbb{E}[S_i]$ drop out – see equations (14), (24) for the generalized gradient constraint, and (15), (26) for the generalized curvature constraint. For example, in the case of the generalized gradient constraint this means that even if the limit of $\overline{f_X}(h_1)/a_1^2$ for $a_1 \rightarrow 0$ is not well defined (i.e., for non-differentiable models), the ratio $\overline{\mathcal{S}}_i/\mathbb{E}[S_i] \propto \overline{f_X}(h_1)/F_\lambda(a_1)$ is still well defined. Similarly one can show that the respective ratio for the generalized curvature constraint is also well defined.

Larger values of the exponent β give smaller values of the distance functional for the same number of iterations. The results for the SSRF parameters do not depend on β . Hence, β is a handle on the convergence rate of the optimization and can be set to one.

Multiple “solutions” of the minimization problem for the model parameters can not be ruled out. The distance functional has by definition a single solution in terms of the z_i . However, since the dependence $z_i(\eta_1, \xi, k_c)$ is nonlinear, more than one solutions for (η_1, ξ, k_c) may be possible, or the optimization algorithm may get trapped near local minima. It is acceptable to have more than one solutions corresponding to different types of “reasonable” spatial dependence.

VIII. NUMERICAL SIMULATIONS

Numerical experiments based on simulated samples are conducted to illustrate the performance of the proposed SSRF inference process. The experiments investigate the ability of FGC-SSRFs to model spatial distributions generated based on commonly used theoretical models. The comparisons are based on the covariance function and on cross-validation.

A. Covariance Estimation

Three covariance models are considered:

1. Spherical

$$c_s(\mathbf{r}) = \sigma_x^2 \left\{ 1 - \frac{3}{2} \frac{\|\mathbf{r}\|}{b_s} + \frac{1}{2} \frac{\|\mathbf{r}\|^3}{b_s^3} \right\} \mathbb{1}_{0 \leq \|\mathbf{r}\| \leq b_s},$$

2. Exponential

$$c_e(\mathbf{r}) = \sigma_x^2 \exp(-\|\mathbf{r}\|/b_e),$$

3. Gaussian

$$c_g(\mathbf{r}) = \sigma_x^2 \exp(-\|\mathbf{r}\|^2/b_g^2).$$

A uniform distribution of $n = 200$ sampling locations $\mathbf{s}_1, \dots, \mathbf{s}_n$ on the two-dimensional domain $[0, 5] \times [0, 5]$ is assumed. The simulated data are denoted by $X^{(m)}(\mathbf{s}_i)$, $1 \leq i \leq n$, where $1 \leq m \leq M$, is the *sample index*. The data are generated from a standard Gaussian spatial random field (zero mean and unit variance) using the Cholesky LU decomposition method. The spatial dependence is given by the three models above, with correlation lengths $b_s = 1$ and $b_e = 0.5$, $b_g = 1$. For each covariance model $M = 100$ independent samples are obtained. Each realization differs from the others in both the sampling locations and the values of the field. The triangular kernel with support $[0, 1]$ is used in SSRF parameter estimation for all the samples.

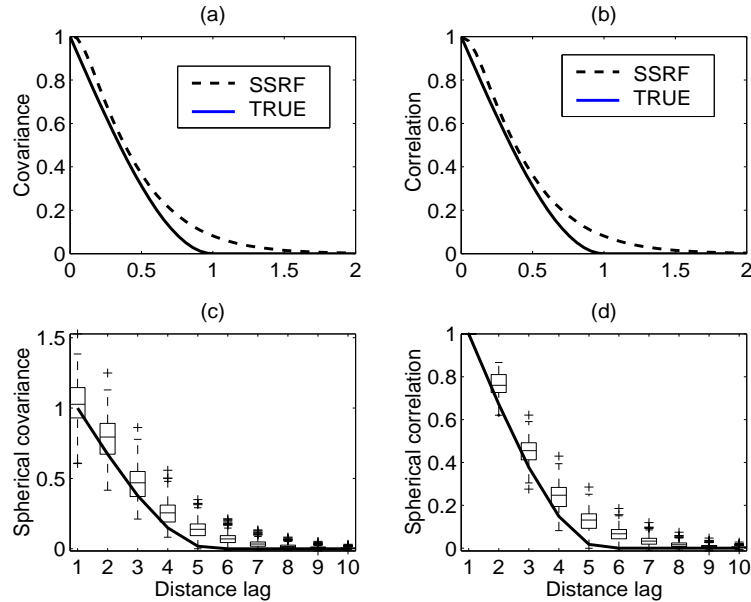


FIG. 1: (a) Spherical covariance (continuous line) and Spartan covariance estimator (broken lines). (c) Box plots of Spartan covariance estimator versus the spherical model. Plots (b) and (d) are the counterparts of plots (a) and (c) respectively for the correlation function.

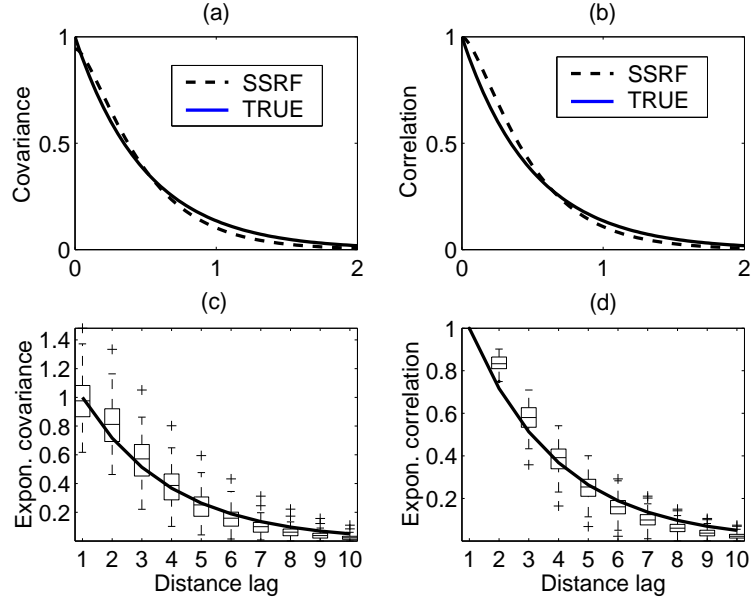


FIG. 2: (a) Exponential covariance (continuous line) and Spartan covariance estimator (broken lines). (c) Box plots of Spartan covariance estimator versus the exponential model. Plots (b) and (d) are the counterparts of plots (a) and (c) respectively for the correlation function.

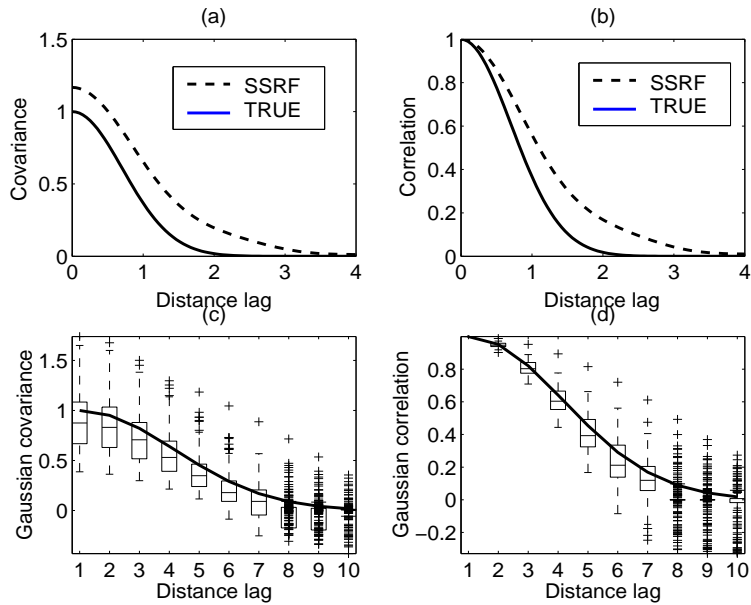


FIG. 3: (a) Gaussian covariance (continuous line) and Spartan covariance estimator (broken lines). (c) Box plots of Spartan covariance estimator versus the Gaussian model. Plots (b) and (d) are the counterparts of plots (a) and (c) respectively for the correlation function.

For each sample, the SSRF covariance estimator is calculated at 10, uniformly spaced intervals between 0 and 1.2. Figure 1 displays the results for simulations based on the spherical model. The covariance function obtained from a single sample is shown for plot (a), and for the correlation function in plot (b). The latter is obtained from the SSRF covariance estimator following division by the sample variance estimate and eliminates the impact of sample-to-sample variance fluctuations. Box plots based on all the samples are shown in plot (c) for the covariance function and in plot (d) for the correlation function. The same plots for the exponential model are shown in Figure 2, and for the Gaussian model in Figure 3. The closer agreement is between the SSRF estimator and the exponential model. This is justified by the fact that in $d = 3$ the SSRF model for $k_c \rightarrow \infty$ and $\eta_1 = 2$ is equivalent to the exponential covariance [12]. The SSRF estimator matches the Gaussian covariance very well near the origin, due to the differentiability of both models. At large lags the SSRF model box plots exhibit considerable scatter, which is due to the fact that for certain realizations the optimization converges to negative η_1 .

It is clear from the plots that the SSRF model does not provide a perfect match with the “true” covariance models over the entire range of lags. However, this is not a major obstacle in geostatistical applications, in which the “true” covariance is unknown. In practice, estimation of the empirical covariance function (or equivalently the variogram) from a single sample involves considerable uncertainties, which are difficult to quantify [20]. The uncertainties are more pronounced at larger lags, at which the averaging procedure involves a smaller number of pairs. Moreover, the theoretical covariance functions merely represent approximations of “actual” covariance functions, and thus do not have any “inherent” advantage over the SSRF model.

B. Cross Validation

In geostatistical applications, the performance of a spatial model is typically evaluated by its ability to “predict” measured sample values at a number of cross validation points. Here we consider $n = 110$ sampling locations over the domain $D = [0, 100] \times [0, 100]$. The set of 110 points is partitioned into a validation set, \mathcal{S}_v , consisting of $n_v = 10$ points chosen at random, and the training set, \mathcal{S}_t , including the remaining $n_t = 100$ points. The two sets of points are shown in Figure 4.

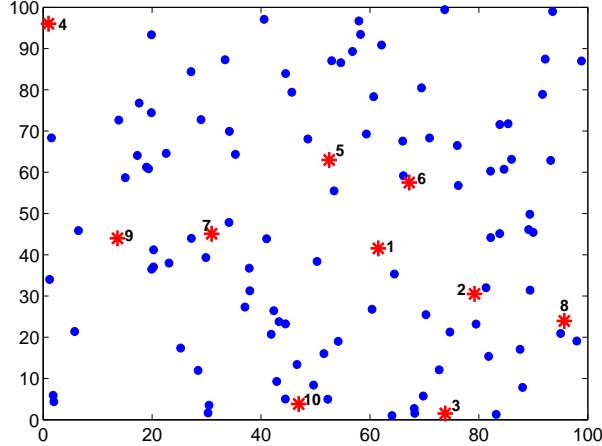


FIG. 4: Locations of the training set (circles) and the validation set (stars).

One hundred independent samples are simulated from a Gaussian SRF with mean $m_X = 70$ and standard deviation $\sigma = 10$ using an exponential covariance model, which will henceforth be referred to as the “true model”. The correlation length is set to $b_e = 4$ (i.e., the correlation range, where the covariance drops to 5% of the initial value is ≈ 12). The true exponential model and the SSRF covariance estimator, obtained from a single sample on \mathcal{S}_t , are given in Figure 5. The behavior of the Spartan estimator follows the plots of Figure (2), that is, the SSRF overestimates the true model near the origin, where it fails to capture the abrupt decline of the exponential.

The performance of the SSRF covariance model is evaluated by means of cross validation. We use the method of Ordinary Kriging, e.g., [5], both with the SSRF covariance and the true exponential covariance to “predict” the field values in \mathcal{S}_v . The predictions based on the SSRF covariance will be denoted by $\hat{X}_{\text{ssrf}}^{(m)}(\mathbf{s}_j)$, while those of the true model with $\hat{X}_{\text{true}}^{(m)}(\mathbf{s}_j)$, $\mathbf{s}_j \in \mathcal{S}_v$; $m = 1, \dots, M$ is the realization (sample) index. In general, a prediction will be denoted by $\hat{X}_t^{(m)}(\mathbf{s}_j)$, where “t=ssrf” for the SSRF model and “t=true” for the true covariance. The relative prediction error is then given by

$$\epsilon_t^{(m)}(\mathbf{s}_j) = \frac{\hat{X}_t^{(m)}(\mathbf{s}_j) - X^{(m)}(\mathbf{s}_j)}{X^{(m)}(\mathbf{s}_j)}. \quad (95)$$

In Table 2 we compare for each point of \mathcal{S}_v the mean relative error (MRE), $\langle \epsilon_{t,1}(\mathbf{s}_j) \rangle = \frac{1}{M} \sum_{m=1}^M \epsilon_t^{(m)}(\mathbf{s}_j)$, and the mean absolute relative error (MARE), $\langle \epsilon_{t,2}(\mathbf{s}_j) \rangle = \frac{1}{M} \sum_{m=1}^M |\epsilon_t^{(m)}(\mathbf{s}_j)|$. The MRE is 5% or lower for both estimators, as expected given the fact that kriging is an unbiased predictor. The MARE is slightly higher for the Spartan model.

This is explained based on the difference between the SSRF and the true covariance function (see Figure 5 below). Note that at \mathbf{s}_4 both models give the same results for the MRE and the MARE. This happens because \mathbf{s}_4 does not have any nearby neighbors, and thus the prediction at this point is reduced to the mean value.

The analysis in this section shows that the SSRF covariance model performs satisfactorily, in terms of cross validation compared to the predictions obtained with the exponential model used to generate the data.

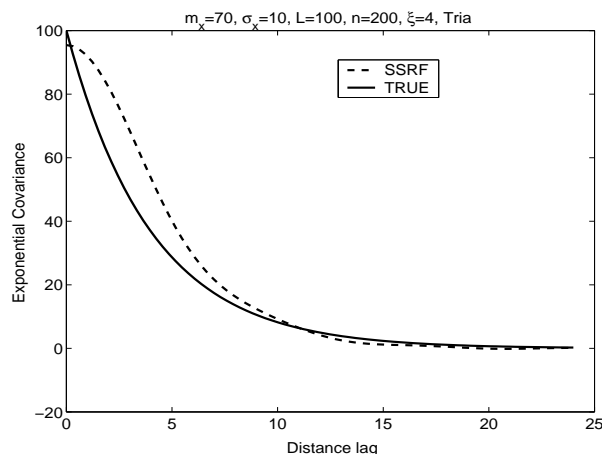


FIG. 5: Comparison of the Spartan covariance estimator (broken line) with the corresponding theoretical model (continuous line).

Acknowledgements

This research is supported by the Marie Curie Action: Marie Curie Fellowship for the Transfer of Knowledge (Project SPATSTAT, Contract No. MTKD-CT-2004-014135) and co-funded by the European Social Fund and National Resources - (EPEAEK-II) PYTHAGORAS.

[1] Armstrong, M. (1998). *Basic Linear Geostatistics*. Springer, Berlin.
 [2] Bochner, S. (1959). *Lectures on Fourier Integrals*. Princeton University Press, Princeton, NJ.
 [3] Christakos, G. (1992). *Random Field Models in Earth Sciences*. Academic Press, San Diego, CA.

Statistics	s_1	s_2	s_3	s_4	s_5	s_6	s_7	s_8	s_9	s_{10}
MRE True	0.0401	0.0038	-0.0040	0.0615	0.0533	-0.0126	0.0192	0.0630	0.0390	0.0075
MRE Spartan	0.0496	0.0043	-0.0147	0.0615	0.0535	-0.0102	0.0096	0.1177	0.0500	0.0075
MARE True	0.1306	0.0961	0.0944	0.1569	0.1456	0.0796	0.1052	0.1064	0.1389	0.0886
MARE Spartan	0.1319	0.1099	0.1344	0.1569	0.1502	0.0848	0.1220	0.1566	0.1552	0.0956

TABLE II: Prediction errors for the Spartan estimator and the true covariance model at the locations in \mathcal{S}_v . First two rows: MRE. Third and fourth rows: MARE. The ordering of the validation points is as shown in Figure (4).

- [4] Christakos, G. and Hristopulos, D. T. (1998). *Spatiotemporal Environmental Health Modelling*. Kluwer, Boston.
- [5] Cressie, N. (1993). *Statistics for Spatial Data*. Wiley, New York.
- [6] Gelhar, L. W. (1993). *Stochastic Subsurface Hydrology*. Prentice Hall, Englewood Cliffs, NJ.
- [7] Goovaerts, P. (1997). *Geostatistics for Natural Resources Evaluation*. Oxford University Press, NY.
- [8] Hall, P., Fischer, N. and Hoffmann, B. (1994) On the nonparametric estimation of covariances functions. *Annals of Statistics*, **22**, 2115-2134.
- [9] Hall, P. and Patil, P. (1994) Properties of nonparametric estimators of autocovariance for stationary random fields. *Probab. Theory Relat. Fields*, **99**, 399-424.
- [10] Hohn, M. E. (1999). *Geostatistics and Petroleum Geology*. Kluwer, Dordrecht.
- [11] Hristopulos, D. T. (2002). New anisotropic covariance models and estimation of anisotropic parameters based on the covariance tensor identity. *Stoch. Environ. Res. and Risk Assessment*, **16**(1), 43-62.

- [12] Hristopulos, D. T. (2003). Spartan Gibbs random field models for geostatistical applications. *SIAM J. Sci. Computing* **24**, 2125-2162.
- [13] Hristopulos, D. T. (2004). Anisotropic Spartan Random Field Models for Geostatistical Analysis. In *Proceedings of 1st International Conference on Advances in Mineral Resources Management and Environmental Geotechnology 2004* (eds Z Agioutantis and K Komnitsas), pp. 127-132. Heliotopos Conferences, Athens.
- [14] Hristopulos, D. T. (2005). Identification of Spatial Anisotropy by means of the Covariance Tensor Identity. In *Mapping radioactivity in the environment: spatial interpolation comparison 2005* (ed. G. Dubois), Office for Official Publications of the European Communities, Luxembourg, in print.
- [15] Hristopulos, D. T. (2005). Spartan gaussian random fields for geostatistical applications: Non-constrained simulations on square lattices and irregular grids. *J. Comput. Methods Sci. Engin.*, **5**(2), 149-164.
- [16] Hristopulos, D. T., and Elogne, S. (2006). Analytic Properties and the covariance function of a class of generalized Gibbs random fields, cs.IT/0605073 (2006).
- [17] Kanevsky, M. and Maignan, M. (2004). *Analysis and Modelling of Spatial Environmental Data*. M. Dekker, New York.
- [18] Kitanidis, P. K. (1997). *Introduction to Geostatistics: Applications to Hydrogeology*. Cambridge University Press, Cambridge.
- [19] Lantuejoul, C. (2001). *Geostatistical Simulation: Models and Algorithms*. Springer, Berlin.
- [20] Marchant, B. P. and Lark, R. M. (2004). Estimating variogram uncertainty. *Math. Geology*, **36**(8), 867-898.
- [21] Nelder, J. A. and Mead, R. (1965). A Simplex Method for Function Minimization. *Comput. J.* **7**, 308-313.
- [22] Rubin, Y. (2003). *Applied Stochastic Hydrogeology*. Oxford University Press, New York.
- [23] Smith, R.L. (2000). Spatial statistics in environmental science. In *Nonlinear and Nonstationary Signal Processing*. (ed. W. J. Fitzgerald, R. L. Smith, A. T. Walden and P. C. Young), pp. 152-183, Cambridge University Press, Cambridge.
- [24] Stein, M.L. (1999). Predicting random fields with increasing dense observations. *Ann. Appl. Probab.*, **9**(1), 242-273.
- [25] Yaglom, A. M. (1987). *Correlation Theory of Stationary and Related Random Functions I:*

Basic Results. Springer, NY.